Radiochim. Acta **100**, 699–713 (2012) / **DOI** 10.1524/ract.2012.1967

Radionuclide behaviour in the near-field of a geological repository for spent nuclear fuel

By V. Metz, H. Geckeis*, E. González-Robles, A. Loida, C. Bube and B. Kienzler

Institute for Nuclear Waste Disposal, Karlsruhe Institute of Technology, Hermann-von-Helmholtz-Platz 1, 76344 Eggenstein-Leopoldshafen, Germany

(Received February 14, 2012; accepted in revised form May 9, 2012)
(Published online July 30, 2012)

UO_2 *fuel corrosion / Radionuclide release / Instant release fraction / Hydrogen effect / Coprecipitation / Sorption*

Summary. Even though chemical processes related to the corrosion of spent nuclear fuel in a deep geological repository are of complex nature, knowledge on underlying mechanisms has very much improved over the last years. As a major result of numerous studies it turns out that alteration of irradiated fuel is significantly inhibited under the strongly reducing conditions induced by container corrosion and consecutive H_2 production. In contrast to earlier results, radiolysis driven fuel corrosion and oxidative dissolution appears to be less relevant for most repository concepts. The protective hydrogen effect on corrosion of irradiated fuel has been evidenced in many experiments. Still, open questions remain related to the exact mechanism and the impact of potentially interfering naturally occurring groundwater trace components. Container corrosion products are known to offer considerable reactive surface area in addition to engineered buffer and backfill material. In combination, waste form, container corrosion products and backfill material represent strong barriers for radionuclide retention and retardation and thus attenuate radionuclide release from the repository near-field.

1. Introduction

Up to 445 000 t of used nuclear fuel from the generation of electricity by nuclear fission are forecasted to accumulate until 2020 [1]. Presently, the vast majority of this high level waste kept in interim storage facilities is irradiated UO_2(s). While the waste amounts normalized to the produced energy are quite low, the high level in radiotoxicity calls for careful treatment and disposal. Only about one third of the worldwide existing used nuclear fuel goes to reprocessing in order to separate U and Pu and to vitrify residual fission products and minor actinides. A number of countries, among those Sweden, Finland, Switzerland and Germany, have decided to directly dispose of irradiated UO_2(s), denoted as Spent Nuclear Fuel (SNF). There is international consensus that disposal in geological formations, such as crystalline rock, clay rock and rock salt, represents the safest way to isolate the high level waste from the biosphere. Transport *via* the groundwater pathway holds as the most relevant mechanism for a potential radionuclide release from the repository and migration towards the biosphere. During the last decades, knowledge on radionuclide behaviour in the near- and far-field of a tentative SNF repository has clearly improved. This is well documented in numerous publications in Radiochimica Acta, where a significant fraction appeared in proceedings papers presented at international MIGRATION conferences. Initial investigations focused on the leaching behaviour of individual radionuclides from SNF under various groundwater conditions in order to derive a kinetic source term applicable to performance assessment modeling [2]. Even though "near-field chemistry" is rather complex, understanding on underlying chemical processes has advanced. The corrosion of waste forms is mainly determined by temperature, groundwater chemistry, radiolysis, and the impact of chemical gradients imposed by fuel and container corrosion and reactions with backfill material. Radionuclide concentrations in the near-field are determined by complexation with groundwater constituents, the solubility of secondary solid phases and temporarily by coupled reaction kinetics and groundwater transport. International concepts rely to a large extent on the enclosure capabilities of the geological barrier in combination with technical and geotechnical barriers. In this context, a clear identification and quantification of radionuclide retention processes in the near-field in case of water access is required. The present paper focuses on progress made concerning insight in chemical near-field reactions of commercial spent UO_2 fuel. Before discussing the experimental studies it is necessary to shortly describe the expected geochemical conditions in the near-field of a deep underground SNF repository.

2. Overview on relevant properties in the near-field of a geological repository

Many countries have initiated research programs to identify suitable geological formations and select potential repository sites for disposal of SNF in a depth of 400 to 1000 m

*Author for correspondence (E-mail: horst.geckeis@kit.edu).
The corresponding author is a member of the Editorial Advisory Board of this journal. Editor

(*e.g.* [3–7]). Besides geological, hydrological, seismic and rock mechanic characteristics of a host formation, its geochemical characteristics determine whether the formation is suitable for disposal of spent nuclear fuel [8]. The selection of potential formations varies among the countries. Depending on the diversity of geological formations present in the countries, crystalline rocks such as granitoids, sedimentary rocks such as plastic or indurated argillites and rock salt complexes are considered. Different engineered barriers have been developed, comprising thick-walled containers for SNF, overpacks, buffer/backfill and plugging materials for the specific requirements defined by the respective geological formations. Detailed descriptions of international final disposal concepts have been presented in recent reviews [9–12]. In the next paragraphs the main characteristics of the various engineered barriers systems for SNF are briefly summarized. In the United States of America, a repository for final disposal of SNF situated within the Yucca Mountain ridge of volcanic tuff was planned. Since the Yucca Mountain Project was halted in March 2010, this disposal system above the groundwater level under oxic conditions is not dealt with in the following.

2.1 Near-field engineered barrier materials

Presently, final disposal in granite, granodiorite or metamorphic bedrocks is under investigation in Canada, Finland, and Sweden, and is also considered by Argentina, China, Czech Republic, Germany, India, Japan, Russia, South Korea and Spain. The Swedish KBS-3 [13, 14] is the most advanced final disposal concept for a crystalline rock formation, and the Finnish and Canadian concepts show great similarities with KBS-3. According to these concepts, SNF will be stored at a depth of about 500 m. Granitoid rock complexes are fractured to some extent and discrete migration pathways will exist therein. Therefore, a cylindrical copper-lined nodular iron (a kind of cast iron) container acts as the main barrier to potential radionuclide release. It is foreseen to embed the container within bentonite, a smectite rich buffer/backfill material, in order to decouple hydraulically the container from the host rock, to prevent the access of groundwater to the container and to provide a significant sorption capacity for radionuclide retention (*e.g.* [15, 16]).

Argillaceous formations are chosen to limit porewater access and solutes migration to slow diffusive transport processes. Due to the high content of smectites and other phyllosilicates, these rocks are characterized by a high sorption and buffer capacity. In Belgium final disposal in plastic clay rocks is investigated, whereas indurated clay rocks are under investigation in France and Switzerland. The latter option is also considered in Argentina, Germany and Spain. The Belgian so-called "Supercontainer" engineered barrier system comprises of containers of SNF assemblies in carbon steel overpacks, which are surrounded by an overpack of a Portland cement concrete buffer and an outer stainless steel envelope [9, 17]. The Swiss disposal concept envisions storage of SNF assemblies in carbon steel overpacks, which will be surrounded by bentonite buffer/backfill material [18, 19]. In France a similar concept has been developed but as the reprocessing technology has been implemented, the primary route is disposal of vitrified high level waste [20].

Disposal of spent nuclear fuel in salt domes and bedded rock salt formations is considered as one option in Germany [12, 21] and discussed as an alternative to the Yucca Mountain Project in the United States of America. Undisturbed rock salt structures are relatively impermeable and virtually free of mobile water; brine reservoirs found within such a salt complex have an almost insignificant volume and do not have any contact to the groundwater in the non-saline geosphere. In Germany, an advanced concept for SNF disposal in rock salt has been developed and examined with respect to safety aspects. The reference concept is based on the so-called POLLUX® container consisting of a stainless steel inner cask and a thick-walled outer cast iron cask to provide shielding. It is planned to use crushed rock salt as backfill and Mg-oxychloride based concrete as plugging materials [22].

2.2 Groundwater compositions

The long-term safety of any of these final disposal systems depends mainly on the extent of interactions of aqueous solutions with the components in the near-field of the waste products. Potential sites for deep underground repositories are characterized by slow water movement or stagnant conditions. The stability of the engineered barrier, of spent nuclear fuel in particular, and the behaviour of mobilized radionuclides depend directly on the composition of the contacting aqueous solution. Beside the influence of the major solution constituents, the effect of HCO_3^- and other minor components is of high concern with respect to complexation of radionuclides and their solubilities.

Formation water compositions have been derived from exploration bore holes and underground research laboratories in granitoid plutons and rock salt complexes ([23–27] and references therein), by means of laboratory leaching and squeezing techniques to extract porewater samples from claystones and bentonites [28–30]. Examples for formation water compositions are presented in [11, 31]. Due to the high residence times of the formation/pore water in the considered bedrocks, the natural solutions are close to saturation with respect to the primary rock-forming minerals or fracture filling materials [31]. At a depth of several hundred meters, investigated argillaceous and granitic type formation waters are Na^+/Cl^- type solutions, characterized by anaerobic conditions and a pH in the range of 7 to almost 9. (Alteration of cement in case of the Belgian "Supercontainer" concept is expected to provide highly alkaline near-field conditions). Low ionic strength ($I < 0.5$ mol $(kg\,H_2O)^{-1}$) formation water is found in potential repository sites and underground research laboratories in Korea, Sweden, Switzerland and Finland (granitoids) as well as in such locations in Belgium, France and Switzerland (argillites), respectively. Formation waters with elevated ionic strength occur in granitic bedrocks in the Canadian Shield and Cretaceous argillites in Northern Germany. Concentrations of major solutes ($Na^+ > Mg^{2+}$, $Ca^{2+} > K^+ > SiO_2(aq) > Fe^{2+}$, $Fe^{3+} > Mn^{2+} > Al^{3+}$ and $Cl^- > SO_4^{2-}$, HCO_3^-, F^-, Br^-) vary significantly between the different sites, reflecting the host specific mineralogical composition. Notably, iron and manganese cations are mainly present in their reduced oxidation state. In contrast to argillaceous and granitic type

formation waters, fluid inclusions and brine pockets in rock salt complexes are characterized by high ionic strengths ($I > 5$ mol (kg H_2O)$^{-1}$), dominated by high concentrations of Na^+, Mg^{2+}, K^+, Cl^- and SO_4^{2-}, to less extent with Ca^{2+}, HCO_3^-, F^- and Br^-. Saline solutions in these host rocks are saturated mainly with halite and anhydrite as well as various chloridic and sulfatic salt mineral assemblages such as halite, kainite, carnallite and sylvite or halite, anhydrite and polyhalite [32–34].

2.3 Geochemical conditions in the near-field

Chemical reactions of the formation water with the host rock, the engineered barrier materials and the spent nuclear fuel itself will alter the water composition and thereby affect the SNF stability and the consecutive radionuclide release. Both kinetic and thermodynamic constraints of alteration reactions of the fuel, container and overpack material as well as radionuclide mobilization and retention depend strongly on the variation of temperature with time. The temperature evolution in the near-field is defined by the radioactive decay of the radionuclides in the waste product, the heat transfer through the walls of container and waste product overpack, the heat conductivity of the backfill and host rock, as well as the spatial dimensions of the emplacement rooms. Peak temperatures are expected to be achieved within decades, reaching values above 100 °C in rock salt repositories (*e.g.* [22, 35]) and significantly below 100 °C in repositories in granitoide rocks (*e.g.* [36]).

Among the various reactions of formation water with the components in the vicinity of the waste, oxidative dissolution (corrosion) of the iron based container material is the key process influencing the radionuclide behaviour in the near-field. In all concepts for final disposal of SNF in deep geological repositories, corrosion of the steel or copper-lined iron [37] containers, failure of containers and water contact with the fuel assemblies are considered [9, 35, 38, 39]. Within few years after closure of a SNF repository, the oxygen content in the backfilled emplacement rooms will be consumed by reactions with the container materials and reducing minerals; additionally biotic respiration/ redox reactions are considered [40–42]. Both at the container/backfill material contact zone and inside a failed SNF container, anaerobic iron corrosion will produce dissolved Fe(II) species, Fe(II)/Fe(III) phases and molecular hydrogen according to Eqs. (1) and (2):

$$Fe + 2H_2O \rightarrow Fe^{2+} + H_2 + 2OH^- \quad (1)$$

$$3Fe + 4H_2O \rightarrow Fe_3O_4(s) + 4H_2 \quad (2)$$

These corrosion reactions establish redox potentials close to – in the long term below – the water stability limit (Fig. 1). While the transition from steel/iron to a thermodynamically stable (hydr)oxide mineral may be debated in terms of transient mineral phases and time scales, there is some agreement that magnetite (Fe_3O_4(s)) is the final product of the corrosion reactions under the conditions of geological waste disposal. Depending on the presence of carbonate and other solutes, Fe(II) phases such as siderite ($FeCO_3$(s)) and mixed Fe(II/III) hydroxide ("green rust") phases can form at least intermediately [43, 44]. Hydrogen produced in the Fe corrosion reaction remains dissolved at considerably high concentrations as long as the pressure built-up in the disposal site does not exceed a minimal principal stress which is defined by the specific geological setting (*i.e.* hydrostatic or lithostatic pressure, respectively). Container corrosion will certainly commence prior to or at the same time as the contact of the solution with the radionuclide containing waste forms within the containers. Consequently, dissolved radionuclide species will interact with iron (hydr)oxide minerals.

3. Alteration of spent nuclear fuel and radionuclide release under repository conditions

Most commercial nuclear fuels used in Light Water Reactors have an initial enrichment of 3 to 5% ^{235}U. So-called mixed-oxide fuel, MOX, contains 5 to 10% ^{239}Pu (originating from reprocessing of irradiated UO_2 fuel) mixed with uranium. Fuel assemblies are rods composed of cylindrical pellets of polycrystalline UO_2(s), which are stacked in tubes of zirconium alloy cladding materials. The pellet diameter is in the order of 1 cm; larger pellets are used for fuel rods

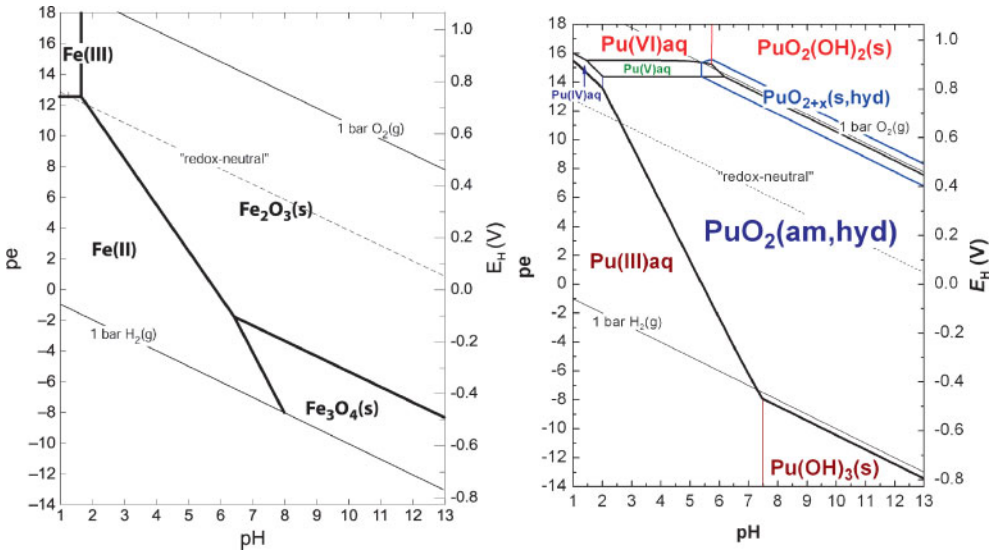

Fig. 1. Simplified redox diagrams of iron (1×10^{-4} mol L^{-1} total Fe concentration; thermodynamic data from Hummel *et al.* [45]) and plutonium (1×10^{-5} mol L^{-1} total Pu concentration); thermodynamic data from the group of Altmaier *et al.* [46, 47] for 0.1 mol L^{-1} NaCl and 25 °C.

in Boiling Water Reactors than in Pressurized Water Reactors. The pellet height is in the range of 1 to 2 cm for fuels of both reactor types [48]. During nuclear reactor operation the UO_2 fuel is subject to intensive transformations due to the fission reactions, the consecutive neutron capture and decay reactions as well as temperature induced transformations (*e.g.* swelling, cracking, diffusion and segregation). After discharge of the fuel from the reactor, the composition of the SNF continues to change with time mainly due to the decay reactions, followed by changes in the thermal and radiation fields. Presently, irradiated fuels with typical burn-ups (BU) of 35 to 45 MW d/(kg UO_2), contain about 95 wt % of UO_2 (mainly ^{238}U, remaining ^{235}U and ^{236}U produced from ^{235}U by neutron capture; *e.g.* [49, 50]). Despite their relatively low content, certain transuranium elements and fission products are highly important with respect to the safety of SNF disposal. In addition to radionuclides in the SNF itself, activation products are present in the cladding. The very intense radiation field of fresh SNF is dominated by short-lived β- and γ-emitters, such as ^{85}Kr, ^{89}Sr, $^{90}Sr/^{90}Y$, ^{91}Y, $^{95}Zr/^{95}Nb$, $^{106}Ru/^{106}Rh$, ^{125}Sb, ^{134}Cs, $^{137}Cs/^{137m}Ba$, $^{144}Ce/^{144}Pr$, ^{147}Pm, and $^{154,155}Eu$. After few hundreds of years most of the β- and γ-emitters will have decayed, and α-emitters ($^{238,239,240}Pu$, $^{241,243}Am$, $^{242,244}Cm$) will dominate the radiation field. The temperature range in the fuel rod decreases from above 1100 °C during reactor operation to some 300 °C during an interim storage period to below 100 °C for thousands of years in the repository. Detailed descriptions of the radionuclide distribution in spent nuclear fuel and the radiochemical properties are given for instance by Kleykamp [51], Carbol *et al.* [11] and Neeb [49].

Dissolution experiments simulating the contact of aqueous solution with SNF demonstrated clearly that the release of radionuclides from the fuel is strongly affected by their spatial distribution among (i) the pellet/ cladding gap region, (ii) grain boundaries, (iii) UO_2 grains/the UO_2 fuel matrix and (iv) in the high burn-up structures/the rim region [50, 52–54]. The alteration of the spent nuclear fuel and the release of radionuclides involve the combination of many different processes, which can be grouped into two stages:

- Fast release of radionuclides at the time of waste package failure. The fraction of quickly released radionuclides is generally referred to as the Fast/Instant Release Fraction (IRF).
- A much slower, long-term radionuclide release that results from the alteration and dissolution of the UO_2 fuel matrix. The reactions of the UO_2 fuel matrix with water are driven both by radiolytic processes and by a thermodynamic affinity effect.

In the following (radio-)chemical properties of SNF, radiolytic reactions in the fuel rod's close vicinity, UO_2 fuel alteration and radionuclide release processes are described.

3.1 (Radio-)chemical and mineralogical properties of spent nuclear fuel

SNF is characterized by a large variety of mixed phase assemblages, a complex distribution of actinides, fission products and distinct structural heterogeneities that result from the fuel's irradiation history, the neutronics, the steep thermal gradient between the pellet's centre and periphery and the initial composition of the fuel. Transuranium elements, fission and activation products occur in many different forms in the spent nuclear fuel. Power ramping and other thermal excursions during reactor operation cause a coarsening of the grain size, extensive microfracturing and migration of fission gases and volatile fission products to grain boundaries, fractures, and the "gap" between the periphery of the fuel pellet and the surrounding cladding. Due to the configuration of the neutron energy spectrum in LWR, there is a higher density of epithermal neutron resonance absorption in ^{238}U nuclei at the radial outer edge ("rim") of the UO_2 fuel pellet, which results in a local enrichment in fissile Pu *via* Np decay and thus in higher local fission density [48, 55]. The local BU at the rim of the UO_2 pellet can be 2–3 times higher than the average pellet BU, depending on the specific irradiation conditions. This spatial increase of BU leads to a microstructure which is characterized by relatively high concentrations of ^{239}Pu, polygonization of the UO_2 grains and thereby a reduction in the size of individual grains.

This microporous structure was already observed in the early 1960's [56] and denoted as "rim structure" corresponding to the position where it was found [57]. In the 1980's there was a renewed interest in the properties of this high burn-up structure due to the increase of the number of irradiation cycles in commercial nuclear power plants. It was demonstrated that the structural changes of the peripheral UO_2 matrix are driven by the radiation damage caused by the accumulation of fission gases and of other fission products in the rim zone [58, 59]. The temperature threshold of the rim zone is 1100 ± 100 °C according to Sonoda *et al.* [59].

According to their chemical and mineralogical properties, Kleykamp *et al.* [60] established a classification for the fission products in SNF. In the past years, this classification has been differentiated further and complemented (see review of Ferry *et al.* [61]).

- Fission gases (Kr, Xe) and other volatile fission products (Br, I and Cs, Rb, Te) which occur as finely dispersed bubbles within UO_2-rich grains, in closed intra-granular and inter-granular bubbles within the fuel matrix [62, 63], and are released to some extent into the plenum of the rod, the open porosity of the fuel and the pellet/cladding gap.
- Metallic fission products (Mo, Tc, Ru, Rh, Pd, Ag, Cd, In, Sn, Sb, Te) forming immiscible, micron- to nanometersized metallic precipitates. These so-called ε-particles are solid solutions of ε-Ru(Mo, Tc, Rh, Pd) with broad variations in concentrations, ε-Mo(Tc, Ru) and ε-Pd(Ru, Rh) [64].
- Fission products forming oxide precipitates (Rb, Cs, Sr, Ba, Zr, Nb, Mo, Te); these oxides tend to have the general composition $AB[O_3]$ and to adopt a cubic perovskite-type structure with Ba, Sr, and Cs in the A sites and Zr, Mo, U and lanthanides (Ln) in the B sites [60, 65].
- Fission products occurring as oxides in the UO_2 fuel matrix (Cs, Nb, Te, Y, Zr, the earth alkaline elements Sr, Ba, Ra and the lanthanides La, Ce, Pr, Nd, Pm, Sm, Eu). Zr and rare earth elements are partially or completely miscible with UO_2 to form a solid solution.

There are continuous transitions between the four groups, which depend on the BU and consequently on the chemical state and solubilities of the fission products [66]. For example, prominent Sr and Zr isotopes occur as $(Ba,Sr,Zr)O_3$ and $(Ba_{1-x-y}Sr_xCs_y)(U,Pu,Ln,Zr,Mo)O_3$ solid solutions as well as $(U,Sr)O_2$ and $(U,Zr)O_2$ solid solutions in the matrix. Similarly to lanthanides, transuranium elements (Pu, Am, Cm, Np) occur in the UO_2 matrix, where they substitute U.

3.2 Radiolysis of aqueous solution

Emission of strong α-, β- and γ-radiation from SNF to adjacent groundwater causes a radiolytical decomposition of the aqueous solution. Radiolysis of water in the near-field is accompanied by the formation of equimolar amounts of oxidizing and reducing species. With respect to primary radiolysis products, H_2 molecules and too less extent $H^\bullet$ radicals are the main reductants, whereas the main oxidants are H_2O_2 (in a α-radiation field/high linear energy transfer, LET) and $OH^\cdot$ radicals (in a β- and γ-radiation field/low LET) in aqueous solutions of low chloride concentration. In salt brines, H_2 molecules are the main reductants, whereas radiolytic oxidants are dominated by oxo-halogenides, such as HClO (both for high and low LET), OH^- (for high LET) and Cl_2^- (for low LET) [67, 68]. Due to the relatively high reactivity of oxidizing radiolysis products, in particular H_2O_2 or oxohalogenides, compared to the reactivity of the main reducing radiolysis product H_2, essentially an oxidative environment is expected to result from the radiolysis in the close vicinity of SNF (*e.g.* [69]). During the first few hundreds of years of disposal, a strong β- and γ-radiation field will be dominant. Afterwards β- and γ-emitters of SNF will have significantly decayed, whereas high inventories of long-lived α-emitters will persist for a much longer time span (*e.g.* [11]).

Radiolytically produced oxidants are expected to oxidize the relatively stable UO_2(s) matrix of SNF into much more soluble U(VI), as long as concentrations of inhibitors such as H_2 are sufficiently low. From reactor chemistry it is well known that radiolysis gases and especially hydrogen develop protective conditions against further progress of radiolysis in deionized water [70–72]. Besides an electrochemically controlled inhibition of SNF corrosion in presence of H_2, a radiolytically controlled protective hydrogen effect with respect to inhibition of SNF corrosion is considered (see [73] and references therein). Various studies were dedicated to examine the influence of molecular hydrogen on the radiolysis of pure water [71, 74–79]. To the present knowledge, a single reaction accounts for the influence of molecular hydrogen on radiolysis of aqueous solution:

$$^\bullet OH + H_2 = H_2O + H^\bullet \quad (3)$$

Ultimately, this reaction converts oxidizing $^\bullet OH$ radicals into reducing $H^\bullet$ radicals. In a recent pulse radiolysis study, Kelm *et al.* [80] confirmed that H_2 interacts radiation chemically solely with the $^\bullet OH$ radical to produce oxidizing long-lived radiolysis products.

Though Br^- is a minor constituent in groundwater of deep geological formations, it is present in a concentration range relevant for radiolytic processes, *i.e.* up to 10^{-3} mol (kg $H_2O)^{-1}$ in granitic groundwater [23, 81], up to 10^{-4} mol (kg $H_2O)^{-1}$ in argillaceous porewater [82] and up to 10^{-1} mol (kg $H_2O)^{-1}$ in salt brines from deep salt formations [25, 26, 83]. It is known from radiolysis of water that even low concentrations of bromide compete with hydrogen for oxidative radiolytic products and consequently reduces the inhibition effect of hydrogen on radiolytic decomposition [84, 85]. Results of α- and γ-radiolysis experiments as well as density functional theory calculations demonstrate (i) it is not the major constituent Cl^-, but the presence of Br^- traces that dominates formation of radiolytic species [68, 86], and (ii) Br^- concentrations of 10^{-4} to 10^{-3} mol (kg $H_2O)^{-1}$ considerably promote radiolytic decomposition, even at 10^{-2} mol H_2 (kg $H_2O)^{-1}$ [85, 87].

Several reviews and synthesis reports about the radiolytical decomposition of groundwater in deep geological SNF repository and about the radiolytically conveyed UO_2(s) corrosion were published in the past [50, 69, 73, 88–91]. To predict the long term performance of SNF in a deep geological repository the mechanism of the involved radiolytical processes must be understood. This includes not only the processes in pure systems – such as deionized water or (diluted) NaCl solution – but also the influence of possible contaminants and of long lived radiolysis products on groundwater radiolysis (*e.g.* [67, 85, 87, 92]).

3.3 Fast/instant release of radionuclides from spent nuclear fuel

The fraction of radionuclides which is segregated during irradiation to the pellet/cladding gap, fractures in the pellet and also to grain boundaries will be relatively quickly released after breaching of container as well as breaching of cladding and contact of aqueous solution with the SNF. This process is generally referred as Instant/Fast Release Fraction (IRF) and comprehends (i) a release from gap and fractures within a period of weeks and (ii) a slower release from grain boundaries during the first few months, which is still faster than release from the UO_2 matrix. Since these processes occur in parallel in leaching experiments, it is not evident to distinguish between the gap and fracture release from the grain boundary release [88, 89, 93–101]. Nevertheless, leaching experiments with powder samples have been conducted that determine, in principal, the IRF contribution associated to the dissolution of the grain boundaries [97–101].

The degree of segregation of the radionuclides depends on various SNF properties, including those caused by the manufacturing process, in-reactor fuel operating parameters such as linear power rating, burn-up, fuel temperature, ramping processes, and interim storage time. Depending on these SNF properties, the IRF comprises few percent of the inventories of fission gases (Kr and Xe), other volatiles fission products (^{129}I, ^{137}Cs, ^{135}Cs, ^{79}Se) and segregated metals (^{99}Tc, ^{107}Pd, ^{126}Sn) [102]. Additionally, some of the activation products from the cladding and fuel assembly structural materials notably ^{14}C and ^{36}Cl, are considered to be subject to a fast release upon contact with aqueous solution.

The fission gas release (FGR) occurs by diffusion to grain boundaries, grain growth accompanied by grain boundary sweeping, gas bubble interlinkage and intersection of gas bubbles by cracks in the SNF [48, 103]. It is more corre-

lated to the linear heat rating, which depends on the fuel temperature, than to the BU of the SNF [102, 104]. The conditions during irradiation ensure that linear heat ratings are kept low and the fission gas release is minimised. Vesterlund *et al.* [105] and Serna *et al.* [106] measured the fission gas release of PWR fuel rods with BU in the range of 18 to 75 MW d/(kg UO_2). Their results show an instant FGR of less than 1% for fuels with a BU below 40 MW d/(kg UO_2). At higher burn-ups a reduction in the thermal conductivity results in an increase of the fuel temperature during reactor operation, which leads to higher FGR, *e.g.* 1% at 50 MW d/(kg UO_2), 3% at 60 MW d/(kg UO_2) and a 7% at 70 MW d/(kg UO_2) [102, 106, 107]. In the case of BWR, measured FGR values were published by Schrire *et al.* [108] and Matsson *et al.* [109]. Similarly to the release of fission gases from PWR fuel, the FGR is less than 1% for BU below 40 MW d/(kg UO_2). For SNF samples with a BU of 50 MW d/(kg UO_2) FGR values of 2 to 5% were found [108, 109].

A comprehensive review of IRF data derived from leaching experiments was carried out by Johnson *et al.* [102]. In an updated IRF assessment that was recently published [110, 111], IRF values have been significantly decreased compared to the estimated values in [102]. However, these reviews and synthesis reports show that the database is scarce for irradiated UO_2 fuels with a BU above 45 MW d/(kg UO_2). González-Robles [101] performed leaching experiments with four high burn-up fuels irradiated in PWR and BWR at burn-ups of 48, 52, 60 and 53 MW d/(kg UO_2). For these types of SNF he quantified IRF values using cladded SNF pellets, determining a conservative contribution of the cladding/pellet gap and fracture release to the IRF, and quantified IRF values using powder samples, determining the contribution associated to the dissolution of the grain boundaries. The combination of experiments with cladded fuel pellets and those with powder samples allowed González-Robles [101] to distinguish between release from the cladding/pellet gap and fracture on one side and release from grain boundaries on the other side.

During the recent years investigations focused on the possible contribution of HBS to the IRF. Clarens and co-workers performed experiments with SNF powder samples prepared from the central and from the peripheral region of SNF pellets [100, 101, 112, 113]. Their results show unambiguously that the fast/instant release of various fission products from the central part of fuel pellets is higher than the release from the HBS enriched peripheral part. These observations are in agreement with experimental results of Roudil and co-workers [99], who found a relatively low instant release fraction of Cs from the rim of a 60 MW d/(kg UO_2) SNF sample, compared to the best estimate values given in [110]. The results published recently by Johnson *et al.* [114] together with those mentioned above [99–101, 112, 113], suggest that the radionuclides segregated into rim pores are isolated to some extent from the aqueous solution and that SNF matrix dissolution is required for its release. Still, there is no consensus how to define the IRF and to quantify the dependence of the IRF on SNF properties. The initial distribution of volatile radionuclides between the various microstructures in the fuel is not completely understood, in particular for high burn-up fuels.

3.4 Radionuclide release due to corrosion of the UO_2 matrix

The release of matrix bound radionuclides depends on the extent of UO_2(s) corrosion, which is controlled by a competition between radiolytic oxidants and complexing species on one side and inhibitors on the other side. The decay of the SNF activity will lead in the long term to such a low radiation dose that radiolysis is expected to become unable to sustain oxidative dissolution. In the absence of oxidizing radiolysis products, U(IV) solubility controlled fuel matrix dissolution would dominate under the reducing conditions of the near-field. Whether or not radiolysis effects are detrimental to the stability of the SNF matrix depends to a large extent also on the time when the fuel container will fail. In case of container breaching at a stage, when the residual spent nuclear fuel inventory is still in the range of several tens to ten thousands of GBq/(kg UO_2), the UO_2 matrix dissolution and radionuclide release will be governed by radiolytically enhanced processes [111].

Most experimental studies that investigate the effect of activity on SNF matrix dissolution kinetics focus on "old" spent nuclear fuel, which is dominated by α-emitters (*e.g.* [97, 115–121]. Poinssot *et al.* reviewed the large experimental dataset and drew the following major conclusions on the SNF matrix dissolution kinetics [111, 122, 123]:

Spent nuclear fuel alteration rates decrease with decreasing α-activity except for the lowest α-activities for which the rate seems to be controlled by solubility of uranium phases and to be independent of the α-activity.

A specific activity threshold exists below which the α-radiation induced matrix dissolution is negligible. At this threshold there is a transition of radiation induced to U(IV) solubility controlled matrix dissolution.

The effective dose threshold is a purely empirical measure of the competition between oxidants production and subsequent matrix alteration on the one hand, and the consumption of oxidants by the other aqueous ions on the other hand. Based on experiments in deionized water, the activity threshold has been estimated to be in the range of 18–33 GBq/(kg UO_2) [111]. This α-activity range corresponds to spent nuclear fuel ages between 3500 and 55 000 years depending on the burn-up of the SNF.

As discussed above, high hydrogen concentrations will be achieved in the near-field of SNF due to anaerobic iron corrosion. Leaching experiments with SNF samples and non irradiated UO_2(s) as well as radiolysis studies indicate that molecular hydrogen both impedes radiolytic decomposition of the diluted and saline solutions and considerably inhibits corrosion of the UO_2(s) matrix [71, 73, 80, 85, 90, 124–132]. Fig. 2 shows an example of an experimental set-up for studying SNF dissolution under H_2 overpressure.

The beneficial inhibition effect of hydrogen on SNF corrosion was observed in leaching experiments with SNF, α-doped UO_2(s) and so-called SIMFUEL samples in simple groundwater simulates (a summary is given in [73]). These aqueous solutions contain only few constituents, mainly Na^+, Cl^- and HCO_3^-/CO_3^{2-}. Fig. 3 shows two SNF samples recovered from corrosion experiments conducted under Ar and H_2 atmosphere, respectively. While in the corrosion experiment under H_2 overpressure there are no hints for pre-

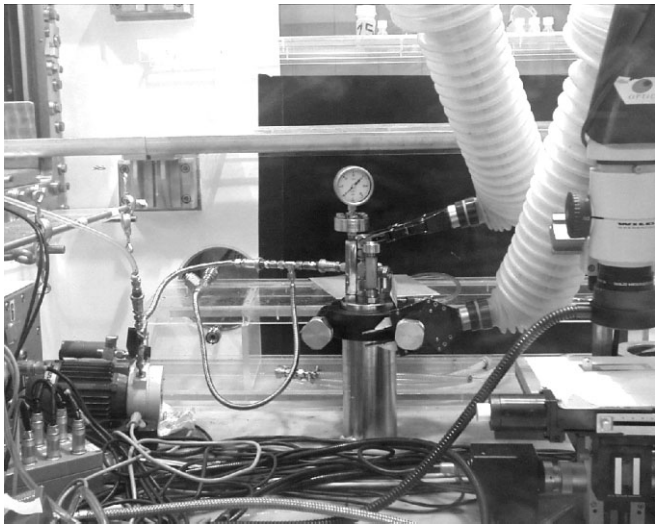

Fig. 2. Corrosion experiment with a spent nuclear fuel sample under H_2 atmosphere in a stainless steel autoclave with titanium liner. H_2 overpressure of 0.3 MPa was achieved by application of 4 MPa Ar-8%H_2 mixture from an external gas supply.

cipitation of secondary U(VI) phases, the surface of the SNF sample corroded under Ar atmosphere is covered with meta-schoepite ($UO_3 : 2H_2O(cr)$).

The protective hydrogen effect is considered to be related to three different electrochemical, radiochemical and radiolytically driven processes [11, 73]:

- Catalytic reactions at the surface of ε-Ru(Mo, Tc, Rh, Pd) and/or other ε-particles;
- UO_2(s) surface controlled reduction of UO_2^{2+}(aq) by H_2 in presence of corroding iron;
- inhibition of the radiolytic production of oxidizing species (H_2O_2 and $OH^{\bullet}$).

Leaching experiments with SNF and UO_2(s) samples as well as electrochemical studies in diluted Na^+-Cl^--HCO_3^-/CO_3^{2-} solutions demonstrate clearly a hydrogen inhibition effect mediated by Ru-Pd-Rh-doping and ε-particles [133–139]. An ε-particle surface mediated hydrogen effect depends on the availability of these particles and might be affected by "poisoning" of these noble metal alloys with dissolved sulfides present in the near-field, whereas a radiolytic driven hydrogen effect will be weakened by counteracting groundwater constituents, such as bromide.

Ollila *et al.* [126] measured dissolution rates of unirradiated UO_2, α-doped UO_2 and SNF in presence of iron. In experiments without ε-particles they observed reduction of U(VI) to U(IV) due to the Fe^{2+} and H_2 produced by iron corrosion. Similarly, Loida *et al.* [125] observed inhibited SNF corrosion in presence of corroding iron in NaCl brine.

Experimental observations regarding the protective hydrogen effect become considerably more complex when investigating interactions of H_2 with SNF/UO_2(s) samples in groundwater simulates which contain minor constituents in addition to Na^+-Cl^--HCO_3^-/CO_3^{2-}. In γ-irradiated 0.1 mol L^{-1} NaCl solution relatively low UO_2(s) corrosion potentials were observed in presence of hydrogen compared to parallel experiments under argon atmosphere, indicating γ-radiolysis induced hydrogen inhibition of UO_2(s) corrosion (see [73, 140] and references therein). In recent experimental studies, SNF dissolution and γ-radiation induced UO_2(s) dissolution were studied at elevated hydrogen pressure in NaCl brine containing 10^{-4} and 10^{-3} mol Br^- (kg $H_2O)^{-1}$ [87, 141]. Similarly to results from SNF dissolution experiment with hydrogen overpressure in absence of hydrogen, measured U concentrations were in the range of the respective solubilities UO_2(am,hyd) at the end of the experiments [125, 129, 141]. The release rate of Sr was significantly increased in the presence of Br^- traces. Both, in the γ-radiolysis experiments with Br^- and without Br^-, the UO_2(s) sample was oxidized, and the concentration of dissolved uranium was controlled by precipitation of secondary U(VI) phases. Oxidation of UO_2(s) in presence of hydrogen in the radiolysis experiments are related to the relatively high γ-dose rate in these experiments. Nevertheless, results of the complementary SNF corrosion and γ-radiolysis experiments allow the conclusion that Br^- traces significantly reduce the protective hydrogen effect with respect to the release of certain radionuclides and the yield of radiolytic products. Published studies on dissolution of UO_2(s) in presence of both hydrogen and bromide were conducted in high β^-/γ- radiation fields, which are relevant to "fresh" spent nuclear fuels. Still, it is unclear whether bromide counteracts the hydrogen inhibition effect on dissolution of thousands years old SNF, which will be dominated by α-emitters after decay of major β^-/γ- emitting fission products. Presently, it is not clear whether ε-particle surface mediated processes, radiolytic processes or the anaerobic H_2/Fe^{2+} production dominates the inhibition effect of hydrogen on SNF corrosion. Still, there is insufficient knowledge about the molecular mechanisms of the protective hydrogen effect on SNF corrosion [132, 141].

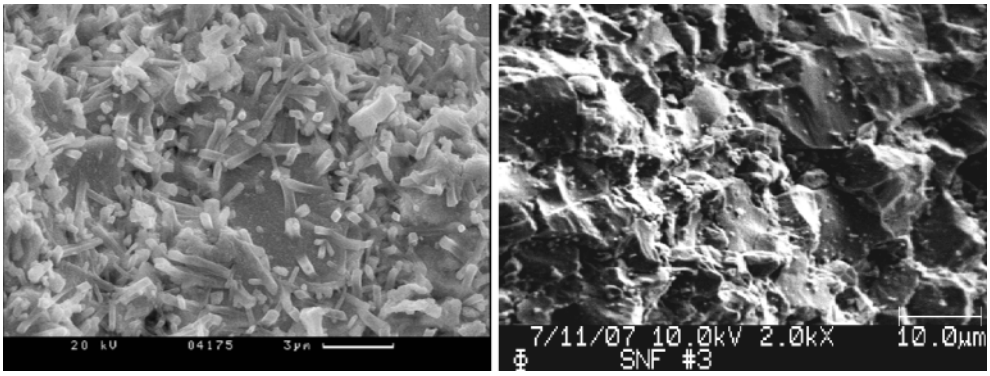

Fig. 3. SNF samples recovered from corrosion experiments under Ar and H_2 atmosphere, respectively. In absence of H_2 overpressure, meta-schoepite precipitated on SNF (left), whereas under H_2 overpressure the UO_2 matrix appears to be free of secondary phases (right; courtesy of E. Ekeroth, Studsvik).

4. Radionuclide retention by coprecipitation and sorption

The solubility of pure solid phases usually is considered as an upper limit for the radionuclide release from SNF. Under 'real' conditions, those concentrations can actually be much lower. Dissolved radionuclides when transported away from the source, may experience coprecipitation with secondary phases, redox reactions, and sorption to surfaces. A multitude of solid phases being formed *in-situ* or initially present in the near-field are conceivable to potentially trap and retain radionuclides and decrease their dissolved concentrations (Table 1).

As UO_{2+x} is main constituent of SNF, secondary forming uranium phases hold as primary hosts for potential radionuclide coprecipitation. Such reactions have been mostly studied in oxidizing environments, which can be expected for radiolytic driven SNF corrosion. Na-polyuranates precipitates containing significant amounts of trivalent lanthanides, Mo, Ba and Th have been found in experiments with carbonate free U(VI) solutions (5 mol L^{-1} NaCl) containing simulated actinide and fission products at variable pH. Tetravalent actinides appear to form pure amorphous oxyhydroxide phases controlling their solubility. Trivalent lanthanides are assumed to form solid solutions with polyuranates [142]. Precipitation experiments with dissolved spent fuel show similar results [148]. Final concentrations of Am, Cm and Eu are lower than expected for the formation of the respective pure hydroxides. Kim *et al.* [143] confirmed those results in own coprecipitation experiments where trivalent lanthanides coprecipitated with various U(VI) hydroxide phases and distribution factors of around 10^3 ml/g are found. Based on crystallographic considerations it has also been shown that actinides in their different oxidation states can in principle be accommodated by U(VI) hydroxide and silicate host matrices [149]. For Np(V) this has been also evidenced by X-ray spectroscopy [150]. The long-lived fission product SeO_3^{2-} is able to replace silicate in secondary U(VI) silicates, while Tc(VII) can not be expected to form mixed solid phases with U(VI) minerals [144]. Metastudite ($UO_4 \cdot 2H_2O$) and studite forming as secondary phases under very oxidizing conditions and intense radiolysis are found to contain ^{90}Sr, ^{137}Cs, and ^{99}Tc in significantly enriched amounts and thus can also be considered to contribute to fission product retention [152].

As discussed before, in deep geological formations as planned for European repository concepts radiolysis driven oxidative dissolution will decrease significantly after several 10 000 years. The establishing reducing conditions amplified by hydrogen evolution from container corrosion will then inhibit SNF corrosion [145] and formation of oxidized uranium secondary phases will become irrelevant (see Fig. 1). Only a few studies are available on the potential formation of coprecipitates of "reduced" secondary uranium phases. Rousseau *et al.* [146] investigated actinide coprecipitation with U(IV) oxide/hydroxides and found formation of $Th_yU_{1-y}O_{2+x}$ (s) and (U, La)O_{2+x} (s) type solid solutions exhibiting lower actinide/lanthanide solubility than expected for the respective pure phases. Whether those findings obtained in laboratory investigations are relevant for the long time evolution of a repository system is not clear. Indications that solid solutions composed of U, Th and Ln oxides are not restricted to laboratory studies are, however, available from natural analogue studies. Natural uraninite samples show highly variable contents of lanthanides, thorium and other elements (mainly Pb) [147]. It is moreover well known that uraninite forms continuous solid solutions with thorianite in nature.

SNF corrosion takes place in presence of corroding or already corroded barrier materials. Those consist in a first instance of corroding/corroded cladding and container material (consisting predominantly of Fe). For the concept of disposal in a thick walled container (*e.g.* POLLUX® with a Fe mass of about 57 t) molar ratios lie at 40–50 : 1 for Fe-U and ∼ 1–2 : 1 for Zr-U. Container material is thus present in large excess over spent fuel. Anaerobic steel corrosion mainly produces magnetite as a finally stable mineral phase and thereby consumes H_2O. Due to different densities of steel and magnetite, the volume of the container material increases by a factor of 1.54 as a result of corrosion and

Table 1. Potential radionuclide retention by coprecipitation with and sorption to solids being present in the near-field of a repository for spent fuel as primary and secondary phases (references are exemplary).

Type of solid phase	Retention mechanisms	Potentially retarded radionuclide
Secondary uranium phases e.g. $UO_4 \cdot 4H_2O$; $Na_2U_2O_7 \cdot 6H_2O$; $UO_3 \cdot 1$–$2H_2O$; $(UO_2)_2SiO_4 \cdot 2H_2O$, $Ca(UO_2)_2(SiO_3OH)_2 \cdot 5H_2O$, UO_2	Coprecipitation, sorption	Actinides [148–152], ^{79}Se [153], Tc(IV) [152], Cs [154], Sr [155]
Cladding corrosion phase: ZrO_2	Coprecipitation, sorption	Actinides [156], Tc [157], Cs [158], Sr [159]
Container corrosion phases: Fe_3O_4, Fe_2O_3, green rust, $Fe(OH)_2$, $FeCO_3$	Coprecipitation, sorption	Actinides [160–169], Cs [170–172], Se [173, 174], Tc [175, 176]
Backfill material: Clay minerals (bentonite); cementitious phases; Sorel phases in case of disposal in rock salt	Sorption	See *e.g.* [29, 178–183]

further reduces the available void volume in the near-field and thus the maximum volume of water which may have access. Corroding steel, therefore, fulfils various barrier functions: it reduces the void volume in emplacement cavities, consumes oxidants and water, ensures reducing conditions, and the generated corrosion products offer extensive reactive surfaces.

Experimental studies on spent fuel corrosion in the presence of corroding iron added as Fe powder [184] showed decreasing concentrations of various radionuclides in SNF leachate solutions notably those of the actinides Am, Cm and Pu. No influence is observed for fission products such as Cs. In case of corroding iron, more than 99% of actinides (except Np) and lanthanides are found associated either to container walls, iron corrosion products and to the SNF surface. In the presence of magnetite alone, more than 70% of the actinides U, Pu and Am were found magnetite-bound and only about 40% of Np. Experiments on the behaviour of uranium added as U(VI) in brine solutions in contact with corroding steel under anaerobic conditions show strong uranium association to solid phases most likely with magnetite after short time period [160]. Such integral studies demonstrate the retention capabilities of iron corrosion products (in particular magnetite), while they do not allow to differentiate between reaction mechanisms either surface sorption, coprecipitation or reduction.

Reduction is highly relevant for the redox sensitive radionuclides U, Np and Tc where poorly soluble tetravalent states establish and for Se where Se^0 or Fe-selenides/sulfides are formed [162, 169, 185]. In case of Pu tri- and tetravalent species may form depending on pH and total Pu concentration (see Fig. 1). Pu(IV) species prevail at high and trivalent species at low pH regions. Solid Pu(IV) hydrous oxide can exist in equilibrium with dissolved Pu(III) species up to pH=10 in presence of corroding iron powder [186]. The solubility of Pu thus increases steeply with decreasing pH. In a recent study, Kirsch *et al.* [163] found very low Pu concentrations in solution in contact with magnetite even though they proved the existence of trivalent species by XANES analysis. Low Pu(III) concentrations are nevertheless maintained by strong sorption to the magnetite surface. The extent of Pu reduction to Pu(III) in presence of Fe(II) was found to depend also on the nature of the final Fe(III) solid due to thermodynamic reasons. Reduction is clearly enhanced in the presence of crystalline goethite [161].

Similarly the reduction of Tc(VII) to Tc(IV) [175, 176] and of Se(VI/IV) to Se^0 and Se^{-2} [187, 188] by Fe(II) containing solid phases have been reported and spectroscopically confirmed. In the case of Se mostly the formation of Se^0 ensures clearly reduced mobility. In addition, formation of $FeSe_x$ and $Fe(S,Se)_x$ phases was found [173, 189]. The potential reduction of U(VI) in presence of magnetite is discussed controversially in the literature [190–192]. Partly no reduction is found, partly the existence of intermediately forming U(V) species is reported. Such observations are usually related to the experimental conditions where even under anaerobic conditions at least partial surfacial oxidation of magnetite cannot be avoided. Complete reduction of U(VI) occurs for molar Fe(II)/Fe(III) ratios x being close to stoichiometric. Magnetite samples with $x \geq 0.38$ reduce U(VI) to UO_2, while solids with $x < 0.38$ do not [193].Natural analogue studies suggest preferential attachment of uranium to iron oxide minerals as *e.g.* observed in mixed weathered mineral assemblages taken from Koongarra (Australia) and Oklo (Gabon) [194].

Bruno *et al.* concluded that a number of trace elements including uranium are incorporated into naturally abundant Fe(III) oxi/hydroxides by an oxidation coprecipitation mechanism [195]. It is however clear that structural compatibility is an important prerequisite for incorporation reactions. In this sense the ionic radii of actinide ions ($r^{VI}(Pu(III)) = 1.00$ Å; $r^{VI}(U(IV)) = 0.89$ Å) are significantly larger than those of Fe ($r^{VI}(Fe(II)) = 0.78$ Å; $r^{VI}(Fe(III)) = 0.785$ Å [196]). This does not mean coprecipitation is excluded entirely. But the induced lattice strains destabilize crystal stability and delimit solid solution formation to the level of trace impurities. Nevertheless, apart from the above mentioned natural analogue studies laboratory experiments revealed spectroscopic evidence for the possible incorporation of trivalent lanthanides into hematite (α-Fe_2O_3(s)) [197]. In case of Tc(IV) full compatibility of technetium with the hematite lattice exists with regard to ionic radii. Quantum chemistry calculations predict energetically favored Tc(IV) incorporation. It is thus not surprising that experiments resulted in Tc(IV) incorporation into the structure of $Fe(OH)_2$ and green rust phases [176].

Fe_3O_4 and ZrO_2 formed by total corrosion of a thick walled container (*e.g.* POLLUX®) and Zircaloy cladding material (~ 3 t Zr) may offer a total amount of surface sites of about 8.8×10^3 mol $>$Fe–OH and 2.4×10^2 mol $\equiv$Zr–OH. Site density data are taken from [156, 198]. Due to interaction of the Zircaloy cladding with hydrogen, formation of Zr hydrides (ZrH_2, ZrH_4) will counteract to some extent any ZrO_2 formation (van Uffelen *et al.*, 2010). To estimate the amount of Fe_3O_4, we assume a void volume of about 140 m^3 per container after a certain degree of compaction in the emplacement gallery backfilled with crushed rock salt (having an intermediate overall porosity of about 10%). These are typical data for a disposal concept in rock salt (Bollingerfehr *et al.*, 2011). Taking an upper limit for U(IV) solubility under reducing conditions including polymeric species of about 10^{-6} mol/L U(IV), a total amount of 1.4×10^{-2} mol uranium per container can dissolve which is about 5–6 orders of magnitude lower than corrosion product surface sites. Sorption at cladding and container corrosion products thus has to be considered as a relevant radionuclide retardation process.

Interaction of a number of radionuclides with magnetite surfaces has been studied and partly surface complexation constants are reported (see Table 1 and references therein). Strong sorption is in general found for tri- and tetravalent actinides but also for hexavalent uranium. Spectroscopic investigations reveal the formation of inner sphere surface complexes mostly bi- or tridentate. EXAFS studies suggest *e.g.* that Th(IV) binds to FeO_6 octahedra and FeO_4 tetraheda in a bidentate fashion [199]. Trivalent actinides such as Pu(III) sorb preferentially at the magnetite (1,1,1) plane as a trifold surface coordinated mononuclear species as concluded from EXAFS [163]. This latter finding fits into general observations of trivalent actinide interaction with oxide minerals (see *e.g.* [200]). Only weak sorption of Cs on pure magnetite is found which however can increase somewhat if

silicate is adsorbed. Adsorbed silicate exerts a bridging effect [171]. Simultaneously sorption of anionic radionuclide species *e.g.* selenite decreases slightly as a consequence of the competing silicate sorption [201]. All studies with magnetite have to be considered with care. Even under anaerobic conditions at least partial surfacial oxidation to maghemite (γ-Fe_2O_3(s)) cannot be excluded (see [193]). We believe there is still research necessary in order to examine the real solid/liquid interface reactions of dissolved radionuclides with magnetite as a function of the Fe(II)/Fe(III) ratio.

Only a few experiments are reported on radionuclide sorption onto ZrO_2. ZrO_2 is well known as inorganic ion exchanger and thus has been proposed for remediation purposes (*e.g.* [157–159]). Sorption of alkali cations has been also performed in order to describe ion behaviour in the primary cycle of nuclear power plants (*e.g.* [202]). Only Simoni *et al.* [156] investigated UO_2^{2+} surface complexation on ZrO_2 and $ZrSiO_4$ by fluorescence spectroscopy and developed surface complexation constants in the context of nuclear waste disposal.

Radionuclide sorption onto near-field corrosion product surfaces must not necessarily reduce the source term for individual waste components. Whether this is the case depends on rates of water transport, container corrosion, SNF dissolution, secondary phase formation and sorption. Scenarios, thus, have to be examined carefully. Radionuclide interaction with corrosion products has been even discussed to possibly enhance SNF dissolution by exerting a pumping effect. Grambow *et al.* [145] concluded that under strongly reducing hydrogen atmosphere, matrix corrosion is very slow so that sorption and dissolution are decoupled and a pumping effect can be excluded. A preliminary simulation of the evolution of a SNF repository in clay rock by a reactive transport model, assuming diffusive transport only, showed that surface interaction with magnetite can have a significant retention effect for the release of actinides such as Am and to a much minor extent also for the retardation of Cs in silicate covered magnetite [203]. Magnetite is predicted to reduce uranium to form uraninite and thus prevents uranium release from the near-field. Similar conclusions have been drawn from a simple simulation of diffusive transport of uranium species through a 0.1 m thick magnetite layer [204].

In addition to sorption and reduction of radionuclides by the container corrosion product layer surrounding the SNF, radionuclide retention will occur at the bentonite buffer and backfill material, which is planned in final disposal concepts for crystalline and argillaceous host rocks. It is well established that the sorption capacity of clay minerals within the geoengineered barrier and the surrounding natural clay eventually retain most of actinides and fission products. Similar conclusions can be drawn for cementitious barriers, as being discussed within the Belgian 'Supercontainer' concept for high-level nuclear waste [205]. Still open is the retention of some long-lived anionic activation and fission products [206]. At least in the presence of alterating cementitious phases, anionic radionuclide species such as $^{36}Cl^-$, $^{129}I^-$, $^{79}SeO_3^{2-}$, and $^{14}CO_3^{2-}$ are reported to undergo significant sorption [181]. Portland cement and alterted cement will not only exist within the Belgian "Supercontainer" concept, but also as construction material in a clay rock repository; $Mg(OH)_2$-$MgCl_2$ based Sorel concrete is foreseen to be present in a repository in rock salt in significant amounts as sealing material and plugs for tunnels. Within the frame of the present paper we do not discuss radionuclide interaction with clay minerals and cementitious material in detail and refer to the literature which is exemplary cited in Table 1.

5. Conclusions

The present paper reviews the current state of knowledge on SNF corrosion in case of groundwater access to the waste form in a repository. A major research outcome during the last decade is the realization that in presence of corroding container material and simultaneous H_2 evolution strongly reducing conditions are established, which considerably influence the stability of SNF and the radionuclide behaviour in the near-field. A number of experimental evidences suggest virtually complete inhibition of UO_2 matrix corrosion in simple hydrogen bearing groundwater simulates. This protective hydrogen effect is related to catalytic or radiolytic activation of molecular hydrogen or related to direct suppression of oxidizing radiolysis products. The role of counteracting groundwater trace components such as Br^- or catalytic poisons *e.g.* sulfide needs to be examined in more detail in order to validate the hydrogen effect. Recent studies confirm moreover strong radionuclide retention by interaction with secondary solid phases derived from SNF alteration but even more pronounced due to reduction, coprecipitation and sorption on container and cladding corrosion products. Mostly these retention processes are not sufficiently quantified and thus often not considered in performance assessment calculations. Such radionuclide retention mechanisms exerted by interaction with corroding materials represent a barrier function in addition to that of engineered barriers such as bentonite and/or cementitious phases. Open questions concern the apparent role of polymeric actinide species in solubility studies. Their potential mobility is not unequivocally ruled out even though filtering can legitimately be assumed in case of nanoporous rock such as clay. Significant retention of the long-lived fission and activation products ^{129}I, ^{36}Cl and ^{14}C in the near-field still has not be proven except in the presence of cement corrosion products.

Acknowledgment. The authors would like to thank Paul Carbol, David Fellhauer, Johannes Lützenkirchen and Thorsten Schäfer for fruitful discussions regarding the impact of hydrogen on SNF corrosion and redox conditions in the near-field of a SNF repository, respectively. The thorough review by an anonymous reviewer is gratefully acknowledged.

References

1. IAEA: Spent fuel reprocessing options. IAEA Technical Reports, IAEA-TECDOC-1587, International Atomic Energy Agency, Vienna (2008).
2. Gray, W. J., Leider, H. R., Steward, S. A.: Parametric study of LWR spent fuel dissolution kinetics. J. Nucl. Mater. **190**, 46 (1992).
3. Bradshaw, R. L.: Ultimate storage of high-level waste solids and liquids in salt formations. In: Proc. Symp. Treatment and Storage of HLW, IAEA, Vienna (1962).
4. Blomeke, J. O., Ferguson, D. E., Croff, A. G.: Disposal of Spent Fuel. Report 780316-4, Oak Ridge National Laboratory (1978).
5. Bradshaw, R. L., Blomeke, J. O., Boegly Jr., W. J., Empson, F. M., Parker, F. L., Perona, J. J., Schaffer Jr., W. F.: Disposal of high activity power reactor wastes in salt mines: a concept and field scale demonstration. Nucl. Struct. Engin. **2**, 438 (1965).

6. Krause, H., Ramdohr, H., Schuchardt, M. C.: Experimental storage of radioactive wastes in the Asse II salt mine. In: Proceedings of a Symposium of Disposal of Radioactive Waste into the Ground, IAEA, Vienna, Austria (1967).
7. Boulton, J.: Management of Radioactive Fuel Wastes: The Canadian disposal Program. Report AECL-6314, Atomic Energy of Canada Limited (1978).
8. Kim, J. I., Grambow, B.: Geochemical assessement of actinide isolation in a German salt repository environment. Engin. Geol. **52**, 221–230 (1999).
9. Bennett, D. G., Gens, R.: Overview of European concepts for high-level waste and spent fuel disposal with reference waste container corrosion. J. Nucl. Mater. **379**, 1 (2008).
10. Falck, W. E., Nilsson, K. F.: Geological disposal of radioactive waste: Moving towards implementation. JRC Reference Report, JRC European Commission, Brussels (2009).
11. Carbol, P., Wegen, D. H., Fors, P.: Spent fuel as waste material. In: *Comprehensive Nuclear Materials*. (Konings, R. J. M., ed.) Elsevier, Amsterdam, Netherlands (2012).
12. Kim, J. S., Kwon, S. K., Sanchez, M., Cho, G. C.: Geological storage of high level nuclear waste. KSCE J. Civil Engin. **15**(4), 721 (2011).
13. SKB: Long-Term Safety for KBS-3 Repositories at Forsmark and Laxemar – A First Evaluation, Main Report of the SR-Can project, SKB TR 06-09, Swedish Nuclear Fuel and Waste Management Co., Stockholm (2006).
14. SKB: Fuel and Canister Process Report for the Safety Assessment SR-Can, SKB TR 06-22. Svensk Kärnbränslehantering AB, Stockholm, Sweden (2006).
15. SKB: SKB Annual Report 1996. SKB TR 96-25. Svensk Kärnbränslehantering AB, Stockholm, Sweden (1997).
16. SKB: Deep repository for long-lived low- and intermediate-level waste. SKB TR 99-28. Svensk Kärnbränslehantering AB, Stockholm, Sweden (1999).
17. Bel, J., Van Cotthem, A., De Bock, C.: Construction, operation and closure of the Belgian repository for long-lived radioactive waste. In: 10th International Conference on Environmental Remediation and Radioactive Waste Management ICEM 2005, Glasgow, UK (2005), p. 1339.
18. NAGRA: Project Opalinus Clay: "Models, Codes and Data for Safety Assessment – Demonstration of disposal feasibility for spent fuel, vitrified high-level waste and long-lived intermediate-level waste (Entsorgungsnachweis)". NAGRA NTB 02-06, Nationale Genossenschaft für die Lagerung radioaktiver Abfälle, Wettingen, Switzerland (2002).
19. NAGRA: Project Opalinus Clay – Safety Report: "Demonstration of Disposal feasibility for spent fuel, vitrified high-level waste and long-lived intermediate level waste (Entsorgungsnachweis)". NAGRA NTB 02-05, Nationale Genossenschaft für die Lagerung radioaktiver Abfälle, Wettingen, Switzerland (2005).
20. ANDRA: Evolution Phenomenologique du Stockage Geologique, 13/520. Tome Evaluation de Surete du Stockage Geologique, 232/737. Dossier 2005 Argile, Agence Nationale pour la Gestion des Déchets Radioactifs, Paris (2005).
21. BGR: *Untersuchung und Bewertung von Regionen mit potenziell geeigneten Wirtsgesteinsformationen*. Bundesanstalt für Geowissenschaften und Rohstoffe (BGR), Hannover (2007).
22. Bollingerfehr, W., Filbert, W., Lerch, C., Tholen, M.: Endlagerkonzepte – Bericht zum Arbeitspaket 5, Vorläufige Sicherheitsanalyse für den Standort Gorleben, GRS-272, Gesellschaft für Anlagen- und Reaktorsicherheit (GRS) (2011).
23. Wittwer, C.: Sondierbohrungen Böttstein, Welach, Riniken, Schafisheim, Kaisten, Leuggern – Probennahmen und chemische Analysen von Grundwässern aus den Sondierbohrungen. NTB 85-49 Report, NAGRA, Wettingen, Switzerland (1986).
24. Guimerà, J., Duro, L., Delos, A.: Changes in groundwater composition as a consequence of deglaciation. SKB R-06-105, Swedish Nuclear Fuel and Waste Management Co., Stockholm, Sweden (2006).
25. Bornemann, O., Behlau, J., Fischbeck, R., Hammer, J., Jaritz, W., Keller, S., Mingerzahn, G., Schramm, M.: Standortbeschreibung Gorleben, Teil 3, Ergebnisse der über- und untertägigen Erkundung des Salinars. Geol. Jr. **C**, 73 (2008).
26. Bornemann, O., Schramm, M., Tomassi-Morawiec, H., Czapowski, G., Misiek, G., Kolonko, P., Janiów, S., Tadych, J.: Wzorcowe profile bromowe cechsztyńskich soli kamiennych w Polsce i w Niemczech na przykładzie kopalni soli w Kłodawie i w Görleben. Standard bromine profiles of the Polish and German Zechstein salts (a case study from the Kłodawa and Görleben salt mines). Geologos **14**, 73 (2008).
27. BfS: Brine Reservoirs in the Gorleben Salt Dome. Bundesamt für Strahlenschutz/Federal Office for Radiation Protection, Salzgitter, http://www.bfs.de/en/endlager/gorleben/loesungen_salzstock.html (2010).
28. Bradbury, M. H., Baeyens, B.: A physicochemical characterisation and geochemical modelling approach for determining porewater chemistries in argillaceous rocks. Geochim. Cosmochim. Acta **62**, 783 (1998).
29. Bradbury, M. H., Baeyens, B.: A physicochemical characterisation and geochemical modelling approach for determining porewater chemistries in argillaceous rocks. J. Contam. Hydrol. **42**, 141 (2000).
30. de Windt, L., Cabrera, J., Boisson, J.-Y.: Radioactive waste containment in indurated shales: comparison between the chemical containment properties of matrix and fractures. In: *Chemical Containment of Waste in the Geosphere*. (Metcalfe, R., Rochelle, C. A., eds.). Geological Society, London (1999).
31. Metz, V., Kienzler, B., Schüßler, W.: Geochemical evaluation of different groundwater-host rock systems for radioactive waste disposal. J. Contam. Hydrol. **61**, 265 (2003).
32. D'Ans, J.: *Die Lösungsgleichgewichte der Systeme der Salze ozeanischer Salzablagerungen*. Verlag Gesellschaft für Ackerbau, Berlin (1933).
33. Braitsch, O.: *Salt deposits, their origin and composition*. Springer Verlag, Berlin (1971), p. 297.
34. Harvie, C. E. Weare, J. H.: The prediction of mineral solubilities in natural waters: the Na-K-Mg-Ca-Cl-SO_4-H_2O system from zero to high concentration at 25 °C. Geochim. Cosmochim. Acta **44**, 981 (1980).
35. Beuth, T., Bracke, G., Buhmann, D., Dresbach, C., Hammer, J., Keller, S., Krone, J., Lommerzheim, A., Mönig, J., Mrugalla, S., Rübel, A., Wolf, J.: Szenarienentwicklung für die Endlagervariante AB1: Kammerlagerung der vernachlässigbar wärmeentwickelnden Abfälle im Südwestflügel und Streckenlagerung der wärmeentwickelnden Abfälle im Nordostflügel des Salzstockes Gorleben, Bericht für Arbeitspaket 8 „Szenarienentwicklung", „Vorläufige Sicherheitsanalyse für den Standort Gorleben", Gesellschaft für Anlagen- und Reaktorsicherheit (GRS) (2012).
36. Duro, L., Grivé, M., Cera, E., Gaona, X., Domènech, C., Bruno, J.: Determination and assessment of the concentration limits to be used in SR-Can. SKB TR-06-32, Swedish Nuclear Fuel and Waste management Co., Stockholm, Sweden (2006).
37. Puigdomenech, I., Ambrosi, J.-P., Eisenlohr, L., Lartigue, J.-E., Banwart, S. A., Bateman, K., Milodowski, A. E., West, J. M., Griffault, L., Gustafsson, E., Hama, K., Yoshida, H., Kotelnikova, S., Pedersen, K., Michaud, V., Trotignon, L., Rivas Perez, J., Tullborg, E.-L.: O_2 depletion in granitic media. SKB TR-01-05, Swedish Nuclear Fuel and Waste Management Co., Stockholm, Sweden (2001).
38. Bowyer, W. H.: A Study of Defects which Might Arise in the Copper Steel Canister, SKI Report 00:19, Swedish Nuclear Power Inspectorate (1999), p. 43.
39. Müller, W., Tholen, M.: Abschätzung der Standzeit von Endlagergebinden in einem zukünftigen HAW-Endlager im Salzgestein unter dem Einfluss der Korrosion. ATW Atomwirtschaft – Atomtechnik **54**, 303 (2009).
40. Wersin, P., Spahiu, K., Bruno, J.: Time evolution of dissolved oxygen and redox conditions in a HLW repository. SKB TR 94-02, Swedish Nuclear Fuel and Waste Management Co., Stockholm, Sweden (1994).
41. Puigdomenech, I., Ambrosi, J.-P., Eisenlohr, L., Lartigue, J.-E., Banwart, S. A., Bateman, K., Milodowski, A. E., West, J. M., Griffault, L., Gustafsson, E., Hama, K., Yoshida, H., Kotelnikova, S., Pedersen, K., Michaud, V., Trotignon, L., Rivas Perez, J., Tullborg, E.-L.: O_2 depletion in granitic media. SKB TR-01-05, Swedish Nuclear Fuel and Waste Management Co., Stockholm, Sweden (2001).

42. Wang, Y., Francis, A. J.: Evaluation of microbial activity for long-term performance assessments of deep geologic nuclear waste repositories. J. Nucl. Radiochem. Sci. **6**, 43 (2005).
43. Johnson, L., King, F.: The effect of the evolution of environmental conditions on the corrosion evolutionary path in a repository for spent fuel and high-level waste in Opalinus Clay. J. Nucl. Mater. **379**, 9 (2008).
44. Martin, F. A., Bataillon, C., Schlegel, M. L.: Corrosion of iron and low alloyed steel within a water saturated brick of clay under anaerobic deep geological disposal conditions: an integrated experiment. J. Nucl. Mater. **379**, 80 (2008).
45. Hummel, W., Berner, U., Curti, E., Pearson, F. J., Thoenen, T.: *Nagra/PSI Chemical Thermodynamic Data Base 01/01*. Universal Publishers, Parkland, FL, USA (2002).
46. Kirsch, R., Fellhauer, D., Altmaier, M., Neck, V., Rossberg, A., Fanghänel, T., Charlet, L., Scheinost, A. C.: Oxidation state and local structure of plutonium reacted with magnetite, mackinawite, and chukanovite. Environ. Sci. Technol. **45**(17), 7267 (2011).
47. Fellhauer, D.: Untersuchungen zur Löslichkeit und Redoxchemie von Np und Pu. Ph. D. thesis, University of Heidelberg, Heidelberg, Germany, in preparation (2012).
48. Van Uffelen, P., Konings, R. M., Vitanza, C., Tulenko, J.: Analysis of reactor fuel rod behavior. In: *Handbook of Nuclear Engineering – Reactor Analysis*. (Cacuci, D. G., ed.) Springer, Heidelberg (2010).
49. Neeb, K.-H.: *The Radiochemistry of Nuclear Power Plants with Light Water Reactors*. De Gruyter, Berlin, Germany (1997), p. 725.
50. Bruno, J., Ewing, R. C.: Spent nuclear fuel. Elements **2**, 343 (2006).
51. Kleykamp, H.: The chemical state of LWR high-power rods under irradiation. J. Nucl. Mater. **84**, 109 (1979).
52. Katayama, Y. B.: Leaching of irradiated LWR fuel pellets in deionized and typical ground water. Report-BNWL-2057, Pacific Northwest Laboratory, Richland, Washington, USA (1976).
53. Johnson, L. H., Garisto, N. C., Stroes-Gascoygne S: Used fuel dissolution studies in Canada. In: Proc. Waste Management '85. (Post, R. G., ed.) Tucson, AZ, USA (1985), p. 479.
54. Poinssot, C., Ferry, C., Kelm, M., Grambow, B., Martinez-Esparza, A., Johnson, L., Adriambololona, Z., Bruno, J., Cachoir, C., Cavedon, J. M., Christensen, H., Corbel, C., Jegou, C., Lemmens, K., Loida, A., Lovera, P., Miserque, F., de Pablo, J., Poulesquen, A., Quinones, J., Rondinella, V. V., Spahiu, K., Wegen, D.: Spent fuel stability under repository conditions – Final Report of the European project. CEA, Saclay, France (2005).
55. Rondinella, V. V., Wiss, T.: The high burn-up structure in nuclear fuel. Mater. Today **13**(12), 24 (2010).
56. Bleiberg, M. L., Berman, R. M., Lustman, B.: Effects of high burn-up on oxide ceramic fuels. In: Proceedings of the Symposium on Radiation Damage in Solids and Reactor Materials, IAEA, Vienna, (1963), p. 319.
57. Klein, D., Baer, W., Smith, G. G.: Spatial distribution of U^{238} resonance neutron capture in uranium metal rods. Nucl. Sci. Eng. **3**, 698 (1958).
58. Walker, C. T.: Assessment of the radial extent and completion of recrystallisation in high burn-up UO_2 nuclear fuel by EPMA. J. Nucl. Mater. **275**(1), 56 (1999).
59. Sonoda, T., Kinoshita, M., Ray, I. L. F., Wiss, T., Thiele, H., Pellotiero, D., Rondinella, V. V., Matzke, H.-J.: Transmission electron microscopy observation on irradiation-induced microstructural evolution in high burn-up UO_2 disk fuel. Nucl. Instrum. Methods B **191**(1–4), 622 (2002).
60. Kleykamp, H., Paschoal, J. O., Pejsa, R., Thümmler, F.: Composition and structure of fission product precipitates in irradiated oxide fuels: Correlation with phase studies in the Mo-Ru-Rh-Pd and BaO-UO_2-ZrO_2-MoO_2 systems. J. Nucl. Mater. **130**, 426 (1985).
61. Ferry, C., Poinssot, C., Broudic, V., Cappelaere, C., Desgranges, L., Garcia, P., Jegou, C., Lovera, P., Marimbeau, P., Piron, J.-P., Poulesquen, A., Roudil, D., Gras, J.-M., Bouffioux, P.: Synthesis on the spent fuel long term evolution. Report CEA-R-6084, Commissariat à L'Énergie Atomique, Saclay, France (2005).
62. Cui, D., Low, J., Sjöstedt, C. J., Spahiu, K.: On Mo-Ru-Tc-Pd-Rh-Te alloy particles extracted from spent fuel and their leaching behaviour under Ar and H_2 atmospheres. Radiochim. Acta **92**, 551 (2004).
63. Walker, C. T., Bremier, S., Portier, S., Hasnaoui, R., Goll, W.: SIMS analysis of an UO_2 fuel irradiated at low temperature to 65 MW d/kg HM. J. Nucl. Mater. **393**, 212 (2009).
64. Kleykamp, H.: Constitution and thermodynamics of the Mo-Ru, Mo-Pd, Ru-Pd and Mo-Ru-Pd systems. J. Nucl. Mater. **167**, 49 (1989).
65. He, H., Keech, P. G., Broczowski, M. E., Noël, J. J., Shoesmith, D. W.: Characterization of the influence of fission product doping on the anodic reactivity of uranium dioxide. Can. J. Chem. **85**, 702 (2007).
66. Kleykamp, H.: The chemical state of the fission products in oxide fuels. J. Nucl. Mater. **131**, 221 (1988).
67. Kelm, M., Bohnert, E.: A kinetic model for the radiolysis of chloride brine, its sensitivity against model parameters and a comparison with experiments. Forschungszentrum Karlsruhe Wissenschaftl. Ber., FZKA 6977, Karlsruhe, Germany (2004).
68. Yamaguchi, M.: Hemibonding of hydroxyl radical and halide anion in aqueous solution. J. Phys. Chem. A **115**, 14620–14628 (2011).
69. Shoesmith, D. W.: Fuel corrosion processes under waste disposal conditions. J. Nucl. Mater. **282**, 1 (2000).
70. Pastina, B., LaVerne, J. A.: Hydrogen peroxide production in the radiolysis of water with heavy ions. J. Phys. Chem. A **103**, 1592 (1999).
71. Pastina, B., LaVerne, J. A.: Effect of molecular hydrogen on hydrogen peroxide in water radiolysis. J. Phys. Chem. A **105**, 9316 (2001).
72. Pastina, B., Isabay, J., Hickel, B.: The influence of water chemistry on the radiolysis of the primary coolant water in pressurized water reactors. J. Nucl. Mater. **264**, 309 (1999).
73. Eriksen, T., Shoesmith, D. W., Jonsson, M.: Radiation induced dissolution of UO_2 based nuclear fuel – a critical review of predictive modelling approaches. J. Nucl. Mater. **420**, 409 (2012).
74. Bunn, D., Dainton, F. S., Salmon, G. A., Hardwick, T. J.: The reactivity of hydroxyl radicals in aqueous solution. Part 2. – Relative reactivities with hydrogen, deuterium and hydrogen deuteride. Trans. Faraday Soc. **55**, 1760–1767 (1959).
75. Schwarz, H. A.: Determination of some rate constants for radical processes in radiation chemistry of water. J. Phys. Chem. **66**, 255–262 (1962).
76. Thomas, J. K.: Rates of reaction of the hydroxyl radical. Trans. Faraday Soc. **61**, 702–707 (1965).
77. Thomas, J. K., Rabani, J., Matheson, M. S., Hart, E. J., Gordon, S.: Absorption spectra of hydroxyl radical. J. Phys. Chem. **70**, 2409–2410 (1966).
78. Christensen, H., Sehested, K.: Reaction of hydroxyl radicals with hydrogen at elevated temperatures. Determination of the activation energy. J. Phys. Chem. **87**, 118–120 (1983).
79. Schmidt, K. H.: Measurement of the activation energy for the reaction of the hydroxyl radical with hydrogen in aqueous solution. J. Phys. Chem. **81**, 1257–1263 (1977).
80. Kelm, M., Metz, V., Bohnert, E., Janata, E., Bube, C.: Interaction of hydrogen with radiolysis products in 0.1 and 1.0 molar NaCl solutions – comparing pulse radiolysis experiments with simulations. Radiat. Phys. Chem. **80**, 426 (2011).
81. Ekberg, C.: Uncertainties in actinide solubility calculations illustrated using the Th-OH-PO4 system. Ph.D. thesis, Chalmers University of Technology, Göteborg, Sweden (1999).
82. Pearson, F. J., Arcos, D., Bath, A., Boisson, J.-Y., Fernandez, A. M., Gäbler, H.-E., Gaucher, E., Gautschi, E., Griffault, L., Hernan, P., Waber, H. N.: Mont Terri Project – geochemistry of water in the Opalinus clay formation at the Mont Terri rock laboratory. BWG Geological Series No. 5, Bundesamt für Wasser und Geologie, Bern (2003).
83. Mattenklott, M.: Die Bromid- und Rubidiumverteilung in Carnallitgesteinen. Univ. Clausthal, Ph.D. thesis, Clausthal-Zellerfeld (1994), p. 214.
84. Henglein, A., Schnabel, W., Wendenburg, J.: *Einführung in die Strahlenchemie*. Verlag Chemie GmbH, Weinheim, Germany (1969).
85. Kelm, M., Bohnert, E.: Gamma radiolysis of NaCl brine: Effect of dissolved radiolysis gases on the radiolytic yield of long-lived products. J. Nucl. Mater. **346**, 1 (2005).

86. Paviet-Hartmann, P., Hartmann, T.: Optimizing nuclear waste repository developments by implementing experimental data on radiolysis. In: Proc. of GLOBAL 2007, Boise, Idaho, USA (2007), p. 691.
87. Metz, V., Bohnert, E., Kelm, M., Schild, D., Reinhardt, J., Kienzler, B., Buchmeiser, M. R.: Gamma-radiolysis of NaCl brine in the presence of UO_2(s): Effects of hydrogen and bromide. Mater. Res. Soc. Symp. Proc. **985**, 33 (2007).
88. Grambow, B., Loida, A., Dressler, P., Geckeis, H., Gago, J., Casas, I., de Pablo, J., Gimenez, J., Torrero, M. E.: Long-Term Safety of Radioactive Waste Disposal: Chemical Reaction of Fabricated and High Burnup Spent UO_2 Fuel with Saline Brines. Forschungszentrum Karlsruhe Wissenschaftl. Ber., FZKA 5702, Karlsruhe, Germany (1996).
89. Grambow, B, Loida, A., Martinez-Esparza, A., Diaz-Arocas, P., de Pablo, J., Paul, J. L., Marx, G., Glatz, J. P., Lemmens, K., Ollila, K.,Christensen, H.: Long-Term Safety of Radioactive Waste Disposal: Source Term for Performance Assessment of Spent Fuel as a Waste Form. Forschungszentrum Karlsruhe Wissenschaftl. Ber., FZKA 6420, Karlsruhe, Germany (2000).
90. Spahiu, K., Werme, L., Eklund, U.-B.: The influence of near field hydrogen on actinide solubilities and spent fuel leaching. Radiochim. Acta **88**, 507 (2000).
91. Spahiu, K., Cui, D., Lundström, M.: The fate of radiolytic oxidants during spent fuel leaching in the presence of dissolved near field hydrogen. Radiochim. Acta **92**, 625 (2004).
92. Gray, W. J.: Gamma Radiolysis of Groundwaters Found near potential Radioactive Waste Repositories, PNL-SA-10928, Pacific Northwest Lab. Richland, WA, USA (1983), p. 10.
93. Wilson, C. N.: Results from NNWSI Series 3 spent fuel dissolution tests. Richland,Washington, USA, Pacific Northwest Laboratory Report PNL-7170 (1990).
94. Wilson, C. N.: Results from NNWSI Series 2 bare fuel dissolution tests. Pacific Northwest Laboratory Report, PNL-7169, Richland, Washington, USA (1990).
95. Forsyth, R. S., Werme, L. O.: Spent fuel corrosion and dissolution. J. Nucl. Mater. **190**, 3 (1992).
96. Forsyth, R. S.: An evaluation of results from the experimental programme performed in the Studsvik Hot Cell Laboratory. SKB Technical Report, TR 97–25, Stockholm, Sweden (1997).
97. Gray, W. J., Wilson, C. N.: Spent fuel dissolution studies FY 1991 to 1994. Technical Report, PNL-10540, Pacific Northwest National Laboratory, Richland, Washington, USA (1995).
98. Kim, S. S., Kang, K. C., Choi, J. W., Seo, H. S., Kwon, S. H., Cho, W. J.: Measurement of the gap and grain boundary inventories of Cs, Sr and I in domestic used PWR Fuels. J. Korean Radioact. Waste Soc. **5**, 79–84 (2007).
99. Roudil, D., Jégou, C., Broudic, V., Tribet, M.: Rim instant release radionuclide inventory from French high burn up spent UOX fuel. Mater. Res. Soc. Symp. Proc. **1193**, 627 (2009).
100. Clarens, F., González-Robles, E., Giménez, F. J., Casas, I., de Pablo, J., Serrano, D., Wegen, D., Glatz, J. P., Martínez-Esparza, A.: Effect of burn-up and high burn-up structure on spent nuclear fuel. ENRESA Publicación Técnica PT-04-09, Madrid, Spain (2009).
101. González-Robles, E.: Study of Radionuclide Release in commercial UO_2 Spent Nuclear Fuel – Effect of Burn-up and High Burn-up Structure. Ph.D. thesis, Universitat Politècnica de Catalunya, Barcelona (2011).
102. Johnson, L., Poinssot, C., Ferry, C., Lovera, P.: Estimates of the Instant Release Fraction for UO_2 and MOX fuel at $t = 0$. Technical Report 04-08, NAGRA, Wettingen, Switzerland (2004).
103. Johnson, L., Shoesmith, D. W.: Spent fuel. In: *Radioactive Waste Forms for the Future*. (Lutze, W., Ewing, R. C., eds.) Elsevier Science Publishers, Amsterdam (1988).
104. Kamikura, K.: FP gas release behaviour of High Burn-up MOX fuel for Thermal Reactors. In: Proc. of Technical Committee Meeting on Fission Gas release and Fuel Rod Chemistry Related to Extended Burnup, IAEA-TEDOC-697, Pembroke, Ontario, Canada (1992), p. 82.
105. Vesterlund, G., Corsetti, L. V.: Recent ABB fuel design and performance experience. In: Proceedings of the 1994 International Topical Meeting on Light Water Reactor Fuel Performance, West Palm Beach, Florida, USA (1994).
106. Serna, J. J., Tolonen, P., Abeta, S., Watanabe, S., Kosaka, Y., Sendo, T., Gonzalez, P.: Experimental observations on fuel pellet performance at high burnup. J. Nucl. Sci. Technol. **43**(9), 1045 (2006).
107. Spino, J., Venix, K., Coquerelle, M.: Detailed characterisation of the rim microstructure in PWR fuels in the burn-up range 40–67 GWd/tM. J. Nucl. Mater. **231**(3), 179 (1996).
108. Schrire, D., Matsson, I., Grapengiesser, B.: Fission gas release in ABB SVEA 10×10 BWR fuel. In: Proceedings of International Topical Meeting on LWR Fuel Performance. American Nuclear Society, La Grange Park, IL, USA (1997), p. 104.
109. Matsson, I., Grapengiesser, B., Andersson, B.: On-site γ-ray spectroscopic measurements of fission gas release in irradiated nuclear fuel. Appl. Radiat. Isotopes **65**(1), 36 (2007).
110. Ferry, C., Piron, J. P., Poulesquen, A., Poinssot, C.: Radionuclides release from the spent fuel under disposal conditions: re-evaluation of the instant release fraction. Mater. Res. Soc. Symp. Proc. **1107**, 447 (2008).
111. Poinssot, C., Gras, J.-M.: Key scientific issues related to the sustainable management of the spent nuclear fuel in the back-end of the fuel cycle. Mater. Res. Soc. Symp. Proc. **1124**, Boston, USA (2009).
112. de Pablo, J., Serrano-Purroy, D., Gonzalez-Robles, E., Clarens, F., Martinez-Esparza, A., Wegen, D., Casas, I., Christiansen, B., Glatz, J. P., Giménez, J.: Effect of HBS structure in fast release fraction of 48 GW d/t U PWR fuel. Proceedings of the 33rd International Symposium on the Scientific Basis for Nuclear Waste Management XXXIII. Mater. Res. Symp. Proc. **1193**, 613–620 (2009).
113. Clarens, F., Serrano-Purroy, D., Martínez-Esparza, A., Wegen, D., González-Robles, E., de Pablo, J., Casas, I., Giménez, J., Christiansen, B., Glatz, J. P.: RN fractional Release of High Burn-Up: Effect of HBS and estimation of accessible grain boundary. Mater. Res. Soc. Symp. Proc. **1107**, 439 (2008).
114. Johnson, L., Günther-Leopold, I., Kobler Waldis, J., Linder, H. P., Low, J., Cui, D., Ekeroth, E., Spahiu, K., Evins, L. Z.: Rapid aqueous release of fission products from high burn-up LWR fuel: Experimental results and correlations with fission gas release. J. Nucl. Mater. **420**, 54 (2012).
115. Bailey, M. G., Johnson, L. H., Shoesmith, D. W.: The effects of alpha radiolysis of water on the corrosion of UO_2. Corros. Sci. **25**, 233 (1985).
116. Stroes-Gascoyne, S., Johnson, L. H., Tait, J. C., McConnell, J. L., Porth, R. J.: Leaching of used CANDU fuel: results from a 19-year leach test under oxidizing conditions. Mat. Res. Soc. Symp. Proc. **465**, 511 (1997).
117. Rondinella, V. V., Matzke, H., Cobos, J., Wiss, T.: Alpha-radiolysis and alpha-radiation damage effects on UO_2 dissolution under spent fuel storage conditions. Mat. Res. Soc. Symp. Proc. **556**, 447 (1999).
118. Rondinella, V. V., Matzke, Hj., Cobos, J., Wiss, T.: Leaching behaviour of UO_2 containing α-emitting actinides, Radiochim. Acta **88**, 527 (2000).
119. Sattonnay, G., Ardois, C., Corbel, C., Lucchini, J. F., Barthe, M. F., Garrido, F., Gosset, D.: Alpha-radiolysis effects on UO_2 alteration in water. J. Nucl. Mater.**288**, 11 (2001).
120. Cobos, J., Havela, L., Rondinella, V. V., de Pablo, J., Gouder, T., Glatz, J. P., Carbol, P., Matzke, H.: Corrosion and dissolution studies of UO_2 containing α-emitters. Radiochim. Acta **90**, 597 (2002).
121. Suzuki, T., Abdelouas, A., Grambow, B., Mennecart, T., Blondiaux, G.: Oxidation and dissolution rates of UO_2(s) in carbonate-rich solutions under external alpha irradiation and initially reducing conditions. Radiochim. Acta **94**, 567 (2006).
122. Poinssot, C., Ferry, C., Lovera, P., Jegou, C., Gras, J.-M.: Spent fuel radionuclide source term model for assessing spent fuel performance in geological disposal. Part II: Matrix alteration model and global performance. J. Nucl. Mater. **346**, 66 (2005).
123. Poinssot, C., Ferry, C., Grambow, B., Kelm, M., Spahiu, K., Martinez, A., Johnson, L., Cera, E., de Pablo, J., Quinones, J., Wegen, D., Lemmens, K., McMenamin, T.: Mechanisms governing the release of radionuclides from spent nuclear fuel in geological repository: major outcomes of the European Project SFS. Mater. Res. Soc. Symp. Proc. **932** (2006).
124. Jegou, C., Muzeau, B., Broudic, V., Peuget, S., Poulesquen, A., Roudil, D., Corbel, C.: Effect of external gamma irradiation on

dissolution of the spent UO_2 fuel matrix. J. Nucl. Mater. **341**, 62 (2005).
125. Loida, A., Metz, V., Kienzler, B., Geckeis, H.: Radionuclide release from high burnup spent fuel during corrosion in salt brine in the presence of hydrogen overpressure. J. Nucl. Mater. **346**, 24 (2005).
126. Ollila, K., Albinsson, Y., Oversby, V. M., Cowper, M.: Dissolution rates of unirradiated UO_2, UO_2 doped with 233U, and spent fuel under normal atmospheric conditions and under reducing conditions using an isotope dilution method. SKB TR-03-13, Swedish Nuclear Fuel and Waste Management Co., Stockholm, Sweden (2003).
127. Carbol, P., Spahiu, K., Cobos-Sabate, J., Glatz, J. P., Ronchi, C., Rondinella, V. V., Wegen, D., Wiss, T., Loida, A., Metz, V., Kienzler, B., Grambow, B., Quinones, J., Martinez-Esparza, A.: The effect of dissolved hydrogen on the dissolution of 233U doped UO_2(s), high burn-up spent fuel and MOX fuel. SKB TR-05-09, Svensk Kärnbränslehantering AB, Stockholm (2005).
128. Carbol, P., Fors, P., Van Winckel, S., Spahiu, K.: Corrosion of irradiated MOX fuel in presence of dissolved H_2. J. Nucl. Mater. **392**, 45 (2009).
129. Carbol, P., Fors, P., Gouder, T., Spahiu, K.: Hydrogen suppresses UO_2 corrosion. Geochim. Cosmochim. Acta **73**, 4366 (2009).
130. Ekeroth, E., Jonsson, M., Eriksen, T., Ljungqvist, K., Kovacs, S., Puigdomenech, I.: Reduction of UO_2^{2+} by H_2. J. Nucl. Mater. **334**, 35 (2004).
131. Cui, D., Ekeroth, E., Fors, P., Spahiu, K.: Surface mediated processes in the interaction of spent fuel or alpha-doped UO_2 with H-2. Mat. Res. Soc. Symp. Proc. **1104**, 87 (2008).
132. Fors, P.: The effect of dissolved hydrogen on spent nuclear fuel corrosion. Ph.D. thesis, Chalmers University of Technology, Göteborg, Sweden (2009).
133. Cui, D., Low, J., Sjöstedt, C. J., Spahiu, K.: On Mo-Ru-Tc-Pd-Rh-Te alloy particles extracted from spent fuel and their leaching behavior under Ar and H_2 atmospheres. Radiochim. Acta **92**, 551 (2004).
134. King, F., Shoesmith, D. W.: Electrochemical studies of the effect of H_2 on UO_2 dissolution. SKB TR-04-20, Swedish Nuclear Fuel and Waste Management Co., Stockholm, Sweden (2004).
135. Broczkowski, M. E., Noel, J. J., Shoesmith, D. W.: The inhibiting effects of hydrogen on the corrosion of uranium dioxide under nuclear waste disposal conditions. J. Nucl. Mater. **346**(1), 16 (2005).
136. Nilsson, S., Jonsson, M.: On the catalytic effect of Pd(s) on the reduction of with H_2 in aqueous solution. J. Nucl. Mater. **374**(1–2), 290 (2008).
137. Nilsson, S., Jonsson, M.: On the catalytic effects of UO_2(s) and Pd(s) on the reaction between H_2O_2 and H_2 in aqueous solution. J. Nucl. Mater. **372**(2–3), 160 (2008).
138. Trummer, M., Roth, O., Jonsson, M.: H_2 inhibition of radiation induced dissolution of spent nuclear fuel. J. Nucl. Mater. **383**(3), 226 (2009).
139. Trummer, M., Nilsson, S., Jonsson, M.: On the effects of fission product noble metal inclusions on the kinetics of radiation induced dissolution of spent nuclear fuel. J. Nucl. Mater. **378**(1), 55 (2008).
140. King, F., Quinn, M. J., Miller, N. H.: The effect of hydrogen and gamma radiation on the oxidation of UO_2 in 0.1 mol dm^{-3} NaCl solution. SKB TR-99-27, Swedish Nuclear Fuel and Waste Management Co., Stockholm, Sweden (1999).
141. Metz, V., Loida, A., Bohnert, E., Schild, D., Dardenne, K.: Effects of hydrogen and bromide on corrosion of spent nuclear fuel and gamma-irradiated UO_2(s) in NaCl brine. Radiochim. Acta **96**, 637 (2008).
142. Diaz Arocas, P., Garcia-Serrano, J., Quinones, J., Geckeis, H., Grambow, B.: Coprecipitation of mono-, di-, tri-, tetra- and hexavalent ions with Na-polyuranates. Radiochim. Acta **74**, 51–58 (1996).
143. Kim, C.-W., Wronkiewicz, D. J., Finch, R. J., Buck, E. C.: Incorporation of cerium and neodymium in uranyl phases. J. Nucl. Mater. **353**, 147–157 (2006).
144. Chen, F., Burns, P. C., Ewing, R. C.: Near-field behavior of ^{99}Tc during the oxidative alteration of spent nuclear fuel. J. Nucl. Mater. **278**, 225–232 (2000).
145. Grambow, B., Giffaut, E.: Coupling of chemical processes in the near field. Mater. Res. Soc. Symp. Proc. **932**, 1067–1074 (2006).
146. Rousseau, G., Fattahi, M., Grambow, B., Boucher, F., Ouvrard, G.: Coprecipitation of thorium and lanthanum with UO_{2+x}(s) as host phase. Radiochim. Acta **94**, 517–522 (2006).
147. Janeczek, J., Ewing, R. C., Oversby, V. M., Werme, L. O.: Uraninite and UO_2 in spent nuclear fuel: a comparison. J. Nucl. Mater. **238**, 121–130 (1996).
148. Quinones, J., Grambow, B., Loida, A., Geckeis, H.: Coprecipitation phenomena during spent fuel dissolution. Part 1: Experimental procedure and initial results on trivalent ion behavior. J. Nucl. Mater. **238**, 38–43 (1996).
149. Burns, P. C., Ewing, R. C., Miller, M. L.: Incorporation mechanisms of actinide elements into the structures of U6+ phases formed during the oxidation of spent nuclear fuel. J. Nucl. Mater. **245**, 1–9 (1997).
150. Burns, P. C., Deely, K. M., Skanthakumar, S.: Neptunium incorporation into uranyl compounds that form as alteration products of spent nuclear fuel: Implications for geologic repository performance. Radiochim. Acta **92**, 151–159 (2004).
151. Douglas, M., Clark, S. B., Friese, J. I., Arey, B. W., Buck, E. C., Hanson, B. D.: Neptunium(V) partitioning to uranium(VI) oxide and peroxide solids. Env. Sci. Technol. **39**, 4117–4124 (2005).
152. McNamara, B., Hanson, B., Buck, E., Soderquist, C.: Corrosion of commercial spent nuclear fuel. 2. Radiochemical analyses of metastudtite and leachates. Radiochim. Acta **93**, 169–175 (2005).
153. Cheng, F. R., Burns, P. C., Ewing, R. C.: ^{79}Se: geochemical and crystallo-chemical retardation mechanisms. J. Nucl. Mater. **275**, 81–94 (1999).
154. Gimenez, J., Martinez-Llado, X., Rovira, M., de Pablo, J., Casas, I., Sureda, R., Martinez-Esparza, A.: Radiochim. Acta **98**, 479–483 (2010).
155. Sureda, R., Martinez-Llado, X., Rovira, M., de Pablo, J., Casas, I., Gimenez, J.: Sorption of strontium on uranyl peroxide: Implications for a high-level nuclear waste repository. J. Hazard. Mater. **181**, 881–885 (2010).
156. Lomenech, C., Drot, R., Simoni, E.: Speciation of uranium(VI) at the solid/solution interface: sorption modeling on zirconium silicate and zirconium oxide. Radiochim. Acta **91**(8), 453–462 (2003).
157. Palmer, D. A., Meyer, R. E.: Adsorption of technetium on selected inorganic ion-exchange materials and on a range of naturally occurring minerals under oxic conditions. J. Inorg. Nucl. Chem. **43**, 2979–2984 (1981).
158. Altas, Y., Tel, H., Yaprak, G.: Sorption kinetics of cesium on hydrous titanium dioxide. Radiochim. Acta **91**, 603–606 (2003).
159. Inan, S., Tel, H., Altas, Y.: Sorption studies of strontium on hydrous zirconium dioxide. J. Radioanal. Nucl. Chem. **267**(3), 615–621 (2006).
160. Grambow, B., Smailos, E., Geckeis, H., Müller, R., Hentschel, D.: Sorption and reduction of uranium(VI) on iron corrosion products under reducing saline conditions. Radiochim. Acta **74**, 149–154 (1996).
161. Felmy, A. R., Moore, D. A., Rosso, K. M., Qafoku, O., Rai, D., Buck, E. C., Ilton, E. S.: Heterogeneous reduction of PuO_2 with Fe(II): importance of the Fe(III) reaction product. Env. Sci. Technol. **45**, 3952–3958 (2011).
162. Christiansen, B. C., Geckeis, H., Marquardt, C. M., Bauer, A., Römer, J., Wiss, T., Schild, D., Stipp, S. L. S.: Neptunyl (NpO_2^+) interaction with green rust, GR(Na,SO_4). Geochim. Cosmochim. Acta **75**, 1216–1226 (2011).
163. Kirsch, R., Fellhauer, D., Altmaier, M., Neck, V., Rossberg, A., Fanghänel, T., Charlet, L., Scheinost, A. C.: Oxidation state and local structure of plutonium reacted with magnetite, mackinawite, and chukanovite. Geochim. Cosmochim. Acta **45**, 7267–7274 (2011).
164. Rojo, I., Seco, F., Rovira, M., Gimenez, J., Cervantes, G., Marti, V., de Pablo, J.: Thorium sorption onto magnetite and ferrihydrite in acidic conditions. J. Nucl. Mater. **385**, 474–478 (2009).
165. Duro, L., El Aamrani, S., Rovira, M., de Pablo, J., Bruno, J.: Study of the interaction between U(VI) and the anoxic corrosion products of carbon steel. Appl. Geochem. **23**, 1094–1100 (2008).
166. Scott, T. B., Allen, G. C., Heard, P. J., Randell, M. G.: Reduction of U(VI) to U(IV) on the surface of magnetite. Geochim. Cosmochim. Acta **69**, 5639–5646 (2005).

167. Missana, T., Maffiotte, U., Garcia-Gutierrez, M.: Surface reactions kinetics between nanocrystalline magnetite and uranyl. J. Coll. Interface Sci. **261**, 154–160 (2003).
168. Cui, D. Q., Spahiu, K.: The reduction of U(VI) on corroded iron under anoxic conditions. Radiochim. Acta **90**, 623–628 (2002).
169. O'Loughlin, E. J., Kelly, S. D., Cook, R. E., Csencsits, R., Kemner, K. M.: Reduction of uranium(VI) by mixed iron(II)/iron(III) hydroxide (green rust): formation of UO_2 nanoparticles. Environ. Sci. Technol. 37, 721–727 (2003).
170. Marmier, N., Delisée, A., Fromage, F.: Surface complexation codeling of Yb(III), Ni(II), and Cs(I) sorption on magnetite. J. Coll. Interface Sci. **211**, 54–60 (1999).
171. Marmier, N., Fromage, F.: Sorption of Cs(I) on magnetite in the presence of silicates. J. Coll. Interface Sci. **223**, 83–88 (2000).
172. Granizo, N., Missana, T.: Mechanisms of cesium sorption onto magnetite. Radiochim. Acta **94**, 671–677 (2006).
173. Scheinost, A. C., Kirsch, R., Banerjee, D., Fernandez-Martinez, A., Zaenker, H., Funke, H., Charlet, L.: X-ray absorption and photoelectron spectroscopy investigation of selenite reduction by Fe(II)-bearing minerals. J. Contam. Hydrol. **102**, 228–245 (2008).
174. Puranen, A., Jonsson, M., Dähn, R., Cui, D. Q.: Reduction of selenite and selenate on anoxically corroded iron and the synergistic effect of uranyl reduction. J. Nucl. Mater. **406**, 230–237 (2010).
175. Llorens, I., Fattahi, M., Grambow, B.: New synthesis route and characterization of siderite ($FeCO_3$) and coprecipitation of ^{99}Tc. In: *Scientific Basis for Nuclear Waste Management*. Materials Research Society **985**, Pittsburg, USA (2007).
176. Llorens, I. A., Deniard, P., Gautron, E., Olicard, A., Fattahi, M., Jobic, S., Grambow, B.: Structural investigation of coprecipitation of technetium-99 with iron phases. Radiochim. Acta **96**, 569 (2008).
177. Bradbury, M. H., Baeyens, B.: A generalised sorption model for the concentration dependent uptake of caesium by argillaceous rocks. J. Cont. Hydrol. **42**, 141–163 (2000).
178. Bradbury, M. H., Baeyens, B.: Predictive sorption modelling of Ni(II), Co(II), Eu(IIII), Th(IV) and U(VI) on MX-80 bentonite and Opalinus Clay: A "bottom-up" approach. Appl. Clay Sci. **52**, 27–33 (2011).
179. Montavon, G., Guo, Z., Lützenkirchen, J., Alhajji, E., Kedziorek, M. A. M., Bourg, A. C. M., Grambow, B.: Interaction of selenite with MX-80 bentonite: Effect of minor phases, pH, selenite loading, solution composition and compaction. Coll. Surf. **332**, 71–77 (2009).
180. Grambow, B., Fattahi, M., Montavon, G., Moisan, C., Giffaut, E.: Sorption of Cs, Ni, Pb, Eu(III), Am(III), Cm, Ac(III), Tc(IV), Th, Zr, and U(IV) on MX 80 bentonite: An experimental approach to assess model uncertainty. Radiochim. Acta **94**, 627–636 (2006).
181. Pointeau, I., Coreau, N., Reiller, P. E.: Uptake of anionic radionuclides onto degraded cement pastes and competing effect of organic ligands, Radiochim. Acta **96**, 367–374 (2008).
182. Paviet-Hartmann, P., Hartmann, T.: Integrated Repository Science for the Long-Term Prediction of Nuclear Waste Disposal, in Nuclear Energy and the Environment (ACS Symposium Series) (2010), Chapt. 27, pp. 381–404.
183. Lützenkirchen, J., Vejmelka, P., Metz, V., Kienzler, B.: Site Specific Sorption Data for the Asse Salt Mine, 9th Int. Conf. Radioactive Waste Management and Environmental Remediation, 4621 (2003), pp. 1–7.
184. Loida, A., Grambow, B., Geckeis, H.: Anoxic corrosion of various high burnup spent fuel samples. J. Nucl. Mater. **238**, 11–22 (1996).
185. Puranen, A., Jonsson, M., Dähn, R., Cui, D.: Reduction of selenite and selenate on anoxically corroded iron and the synergistic effect of uranyl reduction. J. Nucl. Mater. **406**, 230–237 (2010).
186. Altmaier, M., Neck, V., Lützenkirchen, J., Fanghänel, T.: Solubility of plutonium in $MgCl_2$ and $CaCl_2$ solutions in contact with metallic iron. Radiochim. Acta **97**, 187 (2009).
187. Scheinost, A., Kirsch, R., Banerjee, D., Fernandez-Martinez, A., Zaenker, H., Funke, H., Charlet, L.: X-ray absorption and photoelectron spectroscopy investigation of selenite reduction by FeII-bearing minerals. J. Cont. Hydrol. **102**, 228–245 (2008).
188. Skovbjerg, L. L., Christiansen, B. C., Nedel, S., Dideriksen, K., Stipp, S. L. S.: The role of green rust in the migration of radionuclides: An overview of processes that can control mobility of radioactive elements in the environment using as examples Np, Se and Cr. Radiochim. Acta **98**, 607–612 (2010).
189. Liu, X., Fattahi, M., Montavon, G., Grambow, B.: Selenide retention onto pyrite under reducing conditions. Radiochimica Acta **96**, 473 (2008).
190. Missana, T., García-Gutiérrez, M., Fernañdez, V.: Uranium(VI) sorption on colloidal magnetite under anoxic environment: experimental study and surface complexation modeling. Geochim. Cosmochim. Acta **67**, 2543–2550 (2003).
191. Regenspurg, S., Schild, D., Schäfer, T., Huber, F., Malmström, M. E.: Removal of uranium(VI) from the aqueous phase by iron(II) minerals in presence of bicarbonate. Appl. Geochem. **24**, 1617–1625 (2008).
192. Ilton, E. S., Boily, J. F., Buck, E. C., Skomurski, F. N., Rosso, K. M., Cahill, C. L., Bargar, J. R., Felmy, A. R.: Influence of dynamical conditions on the reduction of U(VI) at the magnetite-solution interface. Environ. Sci. Technol. **44**, 170–176 (2010).
193. Latta, D. E., Gorski, C. A., Boyanov, M. I., O'Loughlin, E. J., Kemner, K. M., Scherer, M. M.: Influence of magnetite stoichiometry on UVI reduction. Environ. Sci. Technol. **46**, 778–786 (2012).
194. Lumpkin, G. R., Payne, T. E., Fenton, B. R., Waite, T. D.: Preferential association of adsorbed uranium with mineral surfaces: a study using analytical electron microscopy. Mater. Res. Soc. Symp. Proc. **932**, 1067–1074 (2006).
195. Bruno, J., Duro, L., J. de Pablo, Casas, I., Ayora, C., Delgado, J., Gimeno, M. J., Pena, J., Linklater, C., L. Perez del Villard, Gomez, P.: Estimation of the concentrations of trace metals in natural systems: The application of codissolution and coprecipitation approaches to El Berrocal (Spain) and Pocos de Caldas (Brazil). Chem. Geol. **151**, 277–291 (1998).
196. Shannon, R. D.: Revised effective ionic radii and systematic studies of interatomic distances in halides and chalcogenides. Acta Crystallogr. A **32**, 751–767 (1976).
197. Dardenne, K., Schäfer, T., Lindqvist-Reis, P., Denecke, M. A., Plaschke, M., Rothe, J., Kim, J. I.: Low temperature xafs investigation on the lutetium binding changes during the 2-line ferrihydrite alteration process. Environ. Sci. Technol. **36**, 5092–5099 (2002).
198. Catalette, H., Dumonceau, J., Ollar, P.: Sorption of cesium, barium and europium on magnetite. J. Contamin. Hydrol. **35**, 151–159 (1998).
199. Seco, F., Hennig, C., Pablo de, J., Rovira, M., Rojo, I., Marti, V., Gimenez, J., Duro, L., Grive, M., Bruno, J.: Sorption of Th(IV) onto iron corrosion products: EXAFS study. Environ. Sci. Technol. **43**, 2825–2830 (2009).
200. Polly, R., Schimmelpfennig, B., Rabung, T., Flörsheimer, M., Klenze, R., Geckeis, H.: Quantum chemical study of inner-sphere complexes of trivalent lanthanide and actinide ions on the corundum (0001) surface. Radiochim. Acta, **98**, 627–634 (2010).
201. Jordan, N., Lomenech, C., Marmier, N., Giffaut, E., Ehrhardt, J.-J.: Sorption of selenium(IV) onto magnetite in the presence of silicic acid. J. Coll. Interface Sci. **329**, 17–23 (2009).
202. Palmer, D. A., MacHesky, M. L., Bénézeth, P., Wesolowski, D. J., Anovitz, L. M., Deshon, J. C.: Adsorption of ions on zirconium oxide surfaces from aqueous solutions at high temperatures. J. Solut. Chem. **38**, 907 (2009).
203. De Windt, L., Schneider, H., Ferry, C., Catalette, H., Lagneau, V., Poinssot, C., Poulesquen, A., Jegou, C.: Modeling spent nuclear fuel alteration and radionuclide migration in disposal conditions. Radiochim. Acta **94**, 787–794 (2006).
204. Kienzler, B., Lützenkirchen, J., Bozau, E.: Report on radionuclide source term modelling including test cases for specific conditions, results, improvements and further development. Report: PAMINA Performance Assessment Methodologies in Application to Guide the Development of the Safety Case, European Commission, FP6-036404 (2009).
205. Poyet, S.: The Belgian supercontainer concept: Study of the concrete buffer behaviour in service life. J. Phys. IV France **136**, 167–175 (2006).
206. Grambow, B.: Mobile fission and activation products in nuclear waste disposal. J. Contam. Hydrol. **102**, 180–186 (2008).